UNCLASSIFIED

AD NUMBER
AD208856
LIMITATION CHANGES

TO:

Approved for public release; distribution is unlimited. Document partially illegible.

FROM:

Distribution authorized to U.S. Gov't. agencies and their contractors; Administrative/Operational Use; DEC 1958. Other requests shall be referred to Wright Air Development Center, Wright-Patterson AFB, OH 45433. Document partially illegible.

AUTHORITY
AFFDL ltr, 21 Oct 1974

THIS PAGE IS UNCLASSIFIED

UNCLASSIFIED

AD 208856

Armed Services Technical Information Agency

ARLINGTON HALL STATION
ARLINGTON 12 VIRGINIA

FOR

MICRO-CARD

CONTROL ONLY

1 OF 2

UNCLASSIFIED

WADC TECHNICAL REPORT 58-532

WIND TUNNEL INVESTIGATION OF CONVENTIONAL TYPES OF PARACHUTE CANOPIES IN SUPERSONIC FLOW

R. J. MEYER

COOK RESEARCH LABORATORIES
A DIVISION OF THE COOK ELECTRIC COMPANY
CHICAGO, ILLINOIS

DECEMBER 1958

WRIGHT AIR DEVELOPMENT CENTER

BEST

AVAILABLE

COPY

WIND TUNNEL INVESTIGATION OF CONVENTIONAL TYPES OF PARACHUTE CANOPIES IN SUPERSONIC FLOW

R. A. MEYER

COOK RESEARCH LABORATORIES
A DIVISION OF THE COOK ELECTRIC COMPANY
CHICAGO, ILLINOIS

DECEMBER 1958

WRIGHT AIR DEVELOPMENT CENTER
AIR RESEARCH AND DEVELOPMENT COMMAND
UNITED STATES AIR FORCE
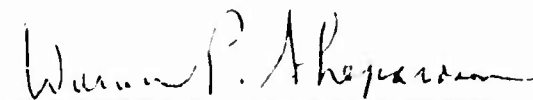WRIGHT-PATTERSON AIR FORCE BASE, OHIO

ABSTRACT

The wind tunnel investigations reported herein are part of an over-all program that has the ultimate goal of achieving a parachute configuration capable of providing satisfactory performance at supersonic speeds. This program has been concerned with the determination of the problems involved and the approaches that should be taken in future test programs such as are being conducted under Contract No. AF 33(616)-5507 with the Air Force. The Lewis phase of the program indicated the following major results; violent canopy breathing or pulsing tendencies and associated reduced inflation and drag characteristics; shock pattern fluctuations which were complicated by interaction effects due to material flexibility; and the failure of ribbons due to violent oscillation of the ribbon fabric. In order to establish the cause of pulsation as evidenced in the Lewis program, a scaled rigid model was utilized in the Langley phase so as to eliminate the interaction effects of flexibility. Although flexibility effects were eliminated by the use of a rigid model at Langley, the fluctuations and discontinuities of the shock patterns were still in evidence. This condition was attributed not only to choking of the flow through the canopy but was also affected by the interaction of the shock front due to choking and disturbances from the confluence point of the lines. It is indicated from the above that future test programs should consider canopies having much increased porosity, particularly in the crown of the canopy. The results of this program also indicate that there is a fundamental shape problem which should be considered in future investigations.

PUBLICATION REVIEW

This report has been reviewed and is approved.

FOR THE COMMANDER:

WARREN P. SHEPARDSON
Chief, Parachute Branch
Aeronautical Accessories Laboratory
Directorate of Laboratories
Wright Air Development Center

TABLE OF CONTENTS

TABLE OF CONTENTS (cont'd)

LIST OF ILLUSTRATIONS

LIST OF TABLES

SECTION I

INTRODUCTION

Since successful recovery of guided missiles or portions of missiles is often necessary and economically advisable, it is desirable to investigate the possibility of recovering such items by the use of parachutes. The use of parachutes in the supersonic regime has become more complicated, however, because the state of the art on parachute design as derived from subsonic tests fails to produce satisfactory configurations for supersonic purposes. Thus, the purpose of the present program has been to investigate the possibility of obtaining a parachute configuration which would be suitable for supersonic operation. The use of a wind tunnel for the establishment of the basic parameter relationships is a logical first approach.

Supersonic wind tunnels capable of simulating performance requirements have been utilized for these investigative purposes. Test programs in the Unitary Plan Wind Tunnels at the Lewis and Langley Research Centers of the NASA were conducted using fabric parachutes at Lewis and rigid, stainless steel models at Langley.

WADC TR 58-532   1

SECTION II

WIND TUNNEL PROGRAM

A. Purpose

The over-all purpose of wind tunnel programs in the Unitary Tunnels at the Lewis and Langley Research Centers was to achieve the most satisfactory parachute configuration for operation at supersonic speeds. Such a configuration would be the one for which flow fluctuations are minimized and the parachute is enabled to perform in a fully inflated condition, producing a steady value of drag force with satisfactory stability. It was realized at this time that the achievement of a satisfactory configuration could not be accomplished within the contractual time limitation. Consequently, arrangements were made with cognizant personnel at WADC, so that the test program could be continued under Contract No. AF 33(616)-5507, which has similar requirements relative to high-speed parachute performance. As a result, this report will discuss the Lewis program and only that portion of the wind tunnel program at Langley which is considered to be relative to the subject contract.

B. Test Facilities

1. The Lewis Research Center Unitary Plan Wind Tunnel

This tunnel, herein referred to as the Lewis wind tunnel, was utilized for the test program of the nearly full-scale fabric parachutes. The tunnel is a facility of the NASA Lewis Research Center at Cleveland, Ohio. The test section is 10 ft x 10 ft in cross section and is capable of a Mach number range of from 2.0 to 3.5. It can be operated throughout the entire Mach number range on either an aerodynamic cycle at various air densities or on a propulsion cycle. On the aerodynamic cycle, the tunnel operates as a closed return type tunnel, and on the propulsion cycle it operates as an open nonreturn type tunnel.

2. The Langley Research Center Unitary Plan Wind Tunnel

The Langley Research Center Unitary Plan Wind Tunnel, which is referred to hereafter in this report as the Langley wind tunnel or facility, was utilized as the test medium for the rigid parachute model. The tunnel is a facility of the NASA, Langley Research Center at Langley Field, Virginia. It has two test sections, each of which is 4 ft x 4 ft in cross section and approximately 7 feet in length. The low

range test section (No. 1) has a design Mach number range of from 1.5 to 2.9 with variation in stagnation pressure possible up to a maximum of approximately 60 psia. The high range test section (No. 2) has a design Mach number range of from 2.3 to 5.0. Its maximum stagnation pressure is approximately 150 psia. Each test section will permit variation of Mach number at any desired increment throughout its range with the tunnel operating. Both stagnation pressure and stagnation temperature may be controlled independently.

C. Test Models and Equipment

1. Fabric Parachute Models (Lewis Test Program)

Two series of fabric parachutes were tested in the wind tunnel at the Lewis Research Center. The first group of nine parachutes was utilized for preliminary or exploratory investigative purposes in an effort to establish criteria upon which designs of final test parachutes could be based. Pertinent characteristics of these parachutes, and those used in the final test program at Lewis, are tabulated in Table 1. Design details are given in Appendix I.

During the preliminary testing phase, parachutes were attached to and deployed behind a 19 inch diameter jet engine inlet upon which scheduled tests were being conducted. All tests were conducted at a Mach number of 3.5 and at a density condition equivalent to an altitude of 70,000 feet. Parachute action during test was recorded photographically by means of Mitchell cameras running at film speeds of 128 frames per second.

Parachutes used in the final test program at Lewis are shown in Table 1. These parachutes incorporated some of the changes and/or improvements which were indicated by the preliminary test program. Installation and deployment of the test parachutes in the test section were accomplished by either of two methods. Most test parachutes were installed according to Installation A of Figure 1; however, for two cases, parachutes were deployed behind a simulated missile body as represented by Installation B in Figure 1.

Most of the test parachutes of this final series were tested at a Mach number of 3.5. Tests of one particular parachute were also conducted at Mach numbers of 2.5 and 2.0 so that the effects of Mach number could be investigated. All tests were conducted at a constant dynamic pressure of 315 psf. Tests utilizing the test setup shown as Installation B in Figure 1 were conducted with the test parachute located 6 and 10 missile diameters respectively behind the simulated missile body.

TABLE 1

PARACHUTE CHARACTERISTICS AND WIND TUNNEL TEST CONDITIONS FOR TEST PROGRAM IN UNITARY PLAN WIND TUNNEL AT THE LEWIS RESEARCH CENTER, CLEVELAND, OHIO

	Parachute Characteristics				Test Conditions			
No	Type	Diameter (ft) (Constructed)	Geometric Porosity (% Total Area)	No. of Gores	Mach No. (M)	Dynamic Pressure (q) (psf)	Reynolds No. (Based on Parachute Diameter ($\times 10^6$)	Remarks
Models Used for Preliminary Test Program								
469	FIST Ribbon	4.25	19.3	8	3.5			
220	Guide Surface Ribless	2.67	10% slots	8	3.5			
472	FIST Ribbon	2.14	26.3	8	3.5			
473	FIST Ribbon	4.11	11.0	8	3.5			
490	FIST Ribbon	4.00	Variable Crown-13.0 Skirt-23.0	8	3.5			
492	FIST Ribbon	4.14	Variable Crown-13.0 Skirt-23.0	8	3.5			
493	FIST Ribbon	4.14	Variable Crown-13.0 Skirt-23.0	8	3.5			Had 1/2 inch rather than 1 inch wide suspension lines
495	FIST Ribbon	4.30	23.0	16	3.5			1/2 scale version of Type 124 parachute developed in sled test
496	Guide Surface Ribless	3.25	No slots	16	3.5			
Models Used in Final Test Program								
513	FIST Ribbon	3.66	19.2	24	3.5	315	1.03	Parachute located 6 missile diameters aft of simulated missile body
514	FIST Ribbon	3.66	19.2	24	3.5	315	1.04	Parachute located 10 missile diameters aft of simulated missile body
508	FIST Ribbon	3.66	19.2	24	3.5	315	1.08	
511	FIST Ribbon	3.66	19.2	24	2.5	315	2.11	
512	FIST Ribbon	3.66	19.2	24	2.0	315	2.69	
507	FIST Ribbon	3.66	Variable Crown-20.0 Skirt-0	16	3.5	315	1.07	
505	FIST Ribbon	4.00	29.4	16	3.5	315	1.14	
506	FIST Ribbon	3.92	5.6	16	3.5	315	1.10	
509	FIST Ribbon	3.66	10.12	24	3.5	315	1.04	
510	Guide Surface Ribless	3.25	20% slots	16	3.5	315	0.92	

Extensive camera coverage was provided. Oblique side views of all test parachutes were achieved by the use of a Mitchell camera running at a speed of 128 frames per second. Schlieren film showing the shock wave patterns of some of the parachutes was obtained by employment of a 1000 frame per second Fastax camera. A third camera, which was installed within a simulated missile body, viewed back into the parachute canopy to film the parachute motions during two high-speed tests. This was a Fairchild camera operated at a film speed of 400 to 500 frames per second.
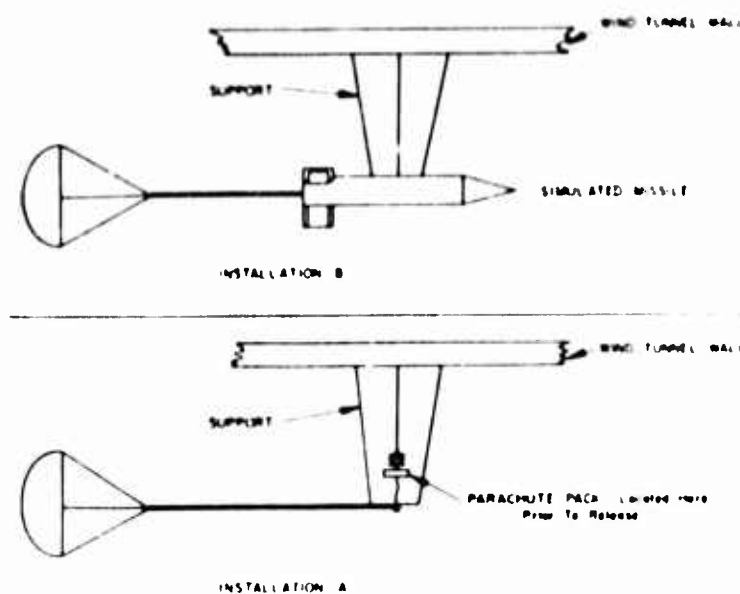
Figure 1. Test Installations - Lewis Unitary Plan Wind Tunnel

2.   Rigid Parachute Models (Langley Test Program)

The continuation of the test program at Langley was the result of a need to consider the effects of flexibility and flow fields on the canopy more fully. Accordingly, a small-scale, stainless steel canopy was designed and constructed for use in the 4 ft x 4 ft Unitary Plan Wind Tunnel at Langley.

The parachute configuration selected for testing in the wind tunnel at Langley was that configuration which exhibited the best performance during the test program at Lewis. This was a 24 gore, 20 percent porosity FIST ribbon parachute. The wind tunnel model was approximately a 1/4 scale rigid version of the fabric parachute. It was constructed of stainless steel to specifications that simulated as closely as possible the configuration of the full-scale fabric parachute. Geometric porosity was attained by appropriate perforation of the canopy. Twenty-four 1/8 inch steel rods, which were utilized to simulate suspension lines, were detachable from the canopy skirt so that changes in suspension line length could be easily made.

Information pertinent to the details of the model design and stress analysis is presented in Appendices II and III, respectively. Typical gore layouts which show the location and geometry of the

slot cutouts are given in Figure 12. Figures 13 and 15 show the test configurations and illustrate the suspension line length variations which were employed.

The model was mounted in the tunnel test section by means of a sting attached to the crown of the canopy as can be seen in the shock photographs presented in Figures 7, 8, or 9. Since flow visualization by means of Schlieren high-speed movies was the ultimate purpose, no balance for obtaining force and moment data was used during these tests. It was felt that efforts to stabilize the flow and minimize the flow fluctuations should be pursued to the utmost before any force measurements were attempted.

SECTION III

DISCUSSION OF TEST RESULTS

A. Fabric Parachute Models (Lewis Test Program)

1. Preliminary Test Program

The purpose of the preliminary testing phase was to attempt to establish criteria upon which the designs of the final test parachutes could be based. In addition, this phase of the program furnished wind tunnel personnel with some idea of the performance characteristics which could be expected from wind tunnel tests of parachutes.

The results of preliminary testing are briefly summarized in the following paragraphs.

Film records for FIST ribbon type parachutes 469, 472 and 473 (see Table 1 for parachute geometry and Appendix I for design details) indicated that porosity variations produced little noticeable improvement in parachute performance. All three specimens experienced failure due to oscillation of horizontal ribbons near the skirt. In each case, the skirt was "breathing" severely at a rate in the order of 50 to 60 cycles. A comparison of ribbon parachutes 469 and 472 revealed nothing significant in the way of "scale" effect in terms of over-all canopy characteristics.

A Guide Surface Ribless parachute (No. 220) failed at the slots after only a few seconds of operation. Progressive canopy failure followed.

Tests of parachutes 490, 492, and 493 failed to show noticeable improvement in the oscillation and pulsing tendencies with changes in skirt porosity and in ribbon spacing. Structural improvements were achieved, however, because of these changes.

A ribbon parachute with variable porosity (No. 493) was designed with 1/2 inch rather than 1 inch wide suspension lines with the expectation of obtaining an indication of the over-all disturbance caused by shock waves from the individual lines stretched out ahead of the canopy.

Parachute 495 was designed as a 1/2 scale version of the most
successful ribbon parachute developed during a sled test program at
Edwards Air Force Base, California. It was a 16 gore, half-scale
version of the Type 124 parachute (Reference 1). Geometric scaling
was carried out in all details. This parachute, with an increased
number of gores, demonstrated some reduction in the oscillation and
pulsing tendencies seen with parachutes 490, 492, and 493.

Parachute 496 proved to be quite stable for a period of 5 seconds
at which time the roof of the canopy failed.

2   Final Test Program

    a.   Test Results

Parachutes used in the final phase at the Lewis facility in-
corporated such changes and/or improvements as were indicated
by the preliminary test program. These parachutes along with
some of their geometric characteristics are tabulated in Table 1.
Design details are presented in Appendix I.

Sufficient test parachutes were available so that the effects
of variations in Mach number, number of gores, and porosity
could be investigated. Ribbon parachutes with 16 and 24 gores
and porosities varying from 5 to 30 percent were utilized. A
variable porosity canopy (see Table 1) incorporating high porosity
at the crown and zero porosity at the skirt was included as one of
the test parachutes. This was because during the preliminary
test phase a large number of failures occurred in the horizontal
ribbons near the skirt. It was suspected that this might be the
result of normal shock movement or buzzing in and out of the
mouth of the canopy. It was anticipated that varying the porosity
distribution over the canopy might reduce buzzing effects.

Guide Surface Ribless type parachutes tested at the Lewis
facility differed mainly in amount of slot opening. In the pre-
liminary phase at Lewis, two Guide Surface Ribless parachutes
with no slots and 10 percent slots, respectively, were tested.
During the final phase at Lewis, 'an additional 20 percent slot
Guide Surface parachute was tested. In all cases, the parachutes
failed at the slots after only a few seconds of operation indicating
that the structural properties of this type of parachute were such
as to prohibit its use for reasonably desirable testing periods.

Tests of the fabric parachutes during the final phase at the Lewis facility indicated that with the exception of Mach number effects, no discernible effects of porosity and number of gores could be ascertained. All tests indicated severe fluctuations in the air flow ahead of a parachute canopy and attendant erratic behavior of the canopy and its drag producing capability.

The phenomena observed during the test program at Lewis indicated the presence of a fluctuating shock pattern ahead of the canopy with a normal shock oscillating between a point adjacent to the parachute skirt and a position somewhat upstream of the canopy. In addition to the normal shock a conical shock was observed which appeared to originate at the point of confluence of the suspension lines. This point of origination at the confluence point could not be confirmed, however, because of the restricted field of view afforded by the Schlieren window

The fluctuation of the shock pattern could be correlated to some degree, with the large magnitude "breathing action" of the parachute canopy with inflation varying from 70 percent of normal inflated diameter to as little as 30 percent of inflated diameter. Typical film sequences, shown in Figures 2 and 3, illustrate the "breathing" or pulsation cycles of four FIST ribbon parachutes as tested at a Mach number of 3.5 during the Lewis wind tunnel program. Parachute inflation and drag characteristics are discussed in greater detail later in this report. In addition to this erratic inflation behavior, a parachute was observed to oscillate with the oscillations becoming more violent as ribbons failed.

The phenomena described above were observed at all Mach numbers but were especially pronounced at the highest test Mach number of 3.5. Somewhat less violent action was indicated at a Mach number of 2.0.

Two factors, acting either independently or simultaneously, were believed to be responsible for the erratic behavior described above. These were:

(1)   The flexibility of conventional parachute materials and structure, which permitted the excessive pulsation of the canopy and lines

(2)   The "shock tickler" effect (References 3 through 6) due to the orientation of the suspension lines and their

Parachute S/N 508M
Diameter 3.66 ft
Porosity 19.2 Percent
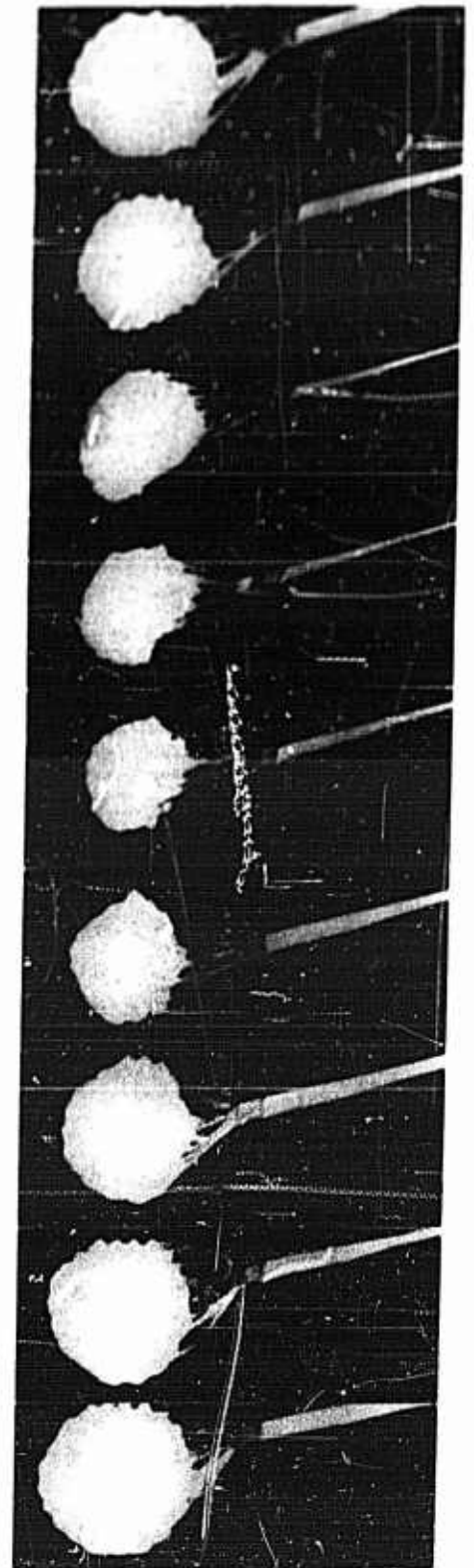
Parachute S/N 509M
Diameter 3.66 ft
Porosity 10.12 Percent

Figure 2. Pulsation Cycles of 24 Gore FIST Ribbon Parachutes
in Wind Tunnel Tests at M = 3.5 (q = 315 psf)

Parachute S/N 505M
Diameter 4 ft
Porosity 29.4 Percent

Parachute S/N 506M
Diameter 3.92 ft
Porosity 5.6 Percent

Figure 3. Pulsation Cycles of 16 Gore FIST Ribbon Parachutes
in Wind Tunnel Tests at M = 3.5 (q = 315 psf)

confluence point upstream of the canopy, which occurs in supersonic flow and tends to place the canopy in a low energy, highly turbulent flow region. For a particular configuration, this action may lead to severe reduction of the parachute drag-producing capability. This factor and its possible influence on parachute drag are discussed in Appendix IV of this report.

It was apparent that the interaction of these two phenomena was complicated and would tend to obscure the configuration characteristics responsible for the observed behavior. Dynamic effects due to the pulsation tendency of the canopy complicated the situation so much that the pressure system which caused the erratic behavior was altered beyond recognition.

b.   Parachute Inflation and Drag Characteristics

Film records of the final tests at the Lewis Research Center indicated that all parachutes tested at a Mach number of 3.5 exhibited rather poor inflation characteristics. The degree of inflation of any test parachute at any time during a test run was difficult to ascertain from the films because of the constant pulsing or breathing action that each parachute experienced during its run. Figures 2 and 3 give some indication of the pulsation cycles of various ribbon test parachutes. It was estimated that the maximum inflation of any ribbon parachute at any time was never greater than about 70 percent of the maximum inflated diameter.

The poor inflation characteristics were further corroborated by the low magnitudes of the recorded drag values provided such values can be treated as absolute values. The validity of these data must be regarded with some suspicion, however, because of difficulties encountered in the response of the measuring system and in the interpretation of the scatter which was present in the Brush records. Although the accuracy of the drag data as shown in Table 2 is questionable, it is believed that such data are sufficiently reliable to warrant the following discussion and/or analysis.

An attempt has been made to correlate the drag coefficients of various ribbon test parachutes with that obtained from a theoretical expression derived in Reference 2. The expression from Reference 2 for the fore drag of a ribbon parachute in dimensionless form and as a function of the inflated area is given by

TABLE 2

DRAG DATA FROM LEWIS WIND TUNNEL TESTS
(q = 315 psf)

Test Run No.	Parachute No.	Geometric Porosity (% Total Area)	Area (ft²) Constructed	Inflated	Mach No.	Drag (lb)	Drag Coefficient (Based on Inflated Area)
1	513	19.2	10.5	4.67	3.5	435	0.296
2	514	19.2	10.5	4.67	3.5	500	0.340
3	508	19.2	10.5	4.67	3.5	450	0.306
4	511	19.2	10.5	4.67	2.5	650	0.442
5	512	19.2	10.5	4.67	2.0	900	0.612
6	507	Variable crown-20.0 skirt-0	10.5	4.67	3.5	350	0.238
7	505	29.4	12.6	5.60	3.5	350	0.198
8	506	5.6	12.1	5.37	3.5	840	0.497
9	509	10.12	10.5	4.67	.5	500	0.340
10	510	20% slots	8.32	8.32	3.5	550	0.210

$$C_{D_N} = \left(K_2 \frac{pt_2}{P_\infty} - 1 \right) \frac{2}{\gamma M^2} \; \sigma_R \; \frac{Ap}{A_o}$$

where

C_{D_N} = fore drag coefficient

K_2 = shape factor = 0.96 (considering a ribbon is a two-dimensional flat plate)

$\dfrac{pt_2}{P_\infty}$ = stagnation pressure after normal shock in terms of free stream static pressure

γ = specific heat ratio = 1.4 (for air)

M = Mach number

$$\sigma_R \quad = \quad \text{parachute solidity factor} \left(1 - \frac{\% \text{ porosity}}{100}\right)$$

$$\frac{A_p}{A_o} \quad = \quad \text{ratio of inflated area to constructed area} = 4/9 \text{ for JIST ribbon parachute}$$

The base drag coefficient of the parachute is given from Reference 2 by

$$C_{D_B} \quad = \quad \frac{2}{\gamma M^2}\left(1 - \frac{P_B}{P_\infty}\right) = \frac{0.83}{M^2}$$

since Reference 2 shows results which indicate an average pressure ratio (P_B/P_∞) value of 0.42 is satisfactory for use over a wide range of supersonic velocities.

Thus, by the use of the above fore and base drag expressions, it has been possible to calculate the total drag coefficients of four ribbon parachutes of different porosity and at Mach numbers for which experimental data were obtained from the Lewis tests. A comparison of these theoretical and experimental values is shown in Figure 4. This figure shows that the agreement between theory and experiment is fair at the lower Mach numbers where the experimental value is approximately 80 percent of the theoretical. This agreement varies with Mach number until at Mach 3.5 the experimental value is only 33 percent of the theoretical. These comparisons have been based on the expected full inflation areas of the parachutes; however, on the basis of a maximum inflation of only 70 percent any agreement such as discussed above must be assumed to be entirely fortuitous.
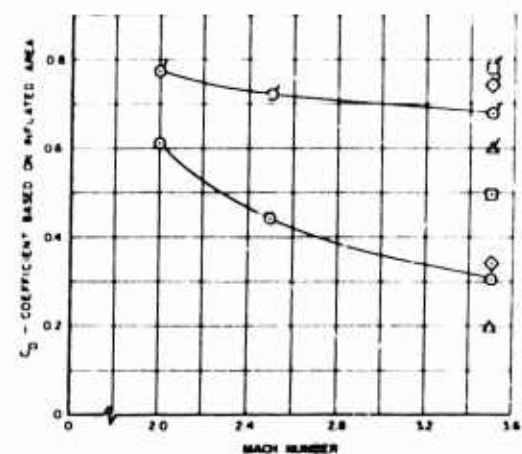

Figure 4. Comparison of Experimental and Theoretical Drag Coefficients (q = 315 psf)

Although some doubt exists with regard to the experimental drag values obtained during the Cleveland tests, enough evidence in the form of motion pictures exists to indicate that the inflation characteristics of the test parachutes at supersonic speeds were extremely poor. Thus, the parachutes were not developing their full drag potential. Further discussion of a possible cause for the reduced drag and inflation characteristics is given in Appendix IV where a comparative analysis of the parachute case with a blunt body - nose spike configuration is considered.

The reduced drag and inflation problems encountered in the Lewis wind tunnel program were also observed in extensive supersonic flight tests as reported in Reference 7. This reference (Reference 7) refers to recovery tests of a supersonic flight test vehicle wherein various test parachutes were utilized as the first or braking stage of a vehicle recovery system. These first stage test parachutes were conical and shaped ribbon parachutes, which were deployed at speeds up to a Mach number of 2.7 at altitudes from 16,000 to 23,000 feet. In addition to reduced drag and poor inflation, these test parachutes exhibited many of the undesirable characteristics which were observed in the Lewis wind tunnel. Among these were: frequent failures of shroud lines at loadings from 1/4 to 1/3 of allowable load; and numerous instances of skirt ribbon failure and flutter.

3. Test Program Continuation

Although the results of the test program in the NASA facility at Cleveland were negative with respect to achievement of a satisfactory parachute configuration, the results served to establish the approach which should be taken in future work. These results indicated that the effects of flexibility on the flow characteristics could be considered more fully by isolating the effects of elasticity. This could be accomplished by utilization of a rigid model in a continuation of the program in a suitable supersonic wind tunnel. Some of the variables which would be considered in a new or continued program would be suspension line length, confluence point location and the apex angle at the confluence point. Accordingly, arrangements for a test program in the Unitary Plan Wind Tunnel at the Langley Research Center of the NASA were finalized.

B.   Rigid Parachute Models

1.   General

Results of the test program in the Langley Research Center Unitary Tunnel were obtained in the form of visual and film observations of the flow patterns about the canopy. Consequently, the following will be limited to a presentation and discussion of these observations as they pertain to particular configurations. A general tabulation of these observations or results is given in Table 3. The configurations tested during this program differed mainly in suspension line length as follows:

(1)   Canopy alone ($\ell/D_o = 0$)

(2)   Canopy plus short suspension line system ($\ell/D_o = 1.0$)

(3)   Canopy plus long suspension line system ($\ell/D_o = 2.0$).

The ℓ/D_o values shown above refer to the suspension line length normal to the canopy skirt in terms of the constructed diameter (12 inches) of the parachute model. The variations listed above are illustrated in Figure 15.

2.   Canopy Alone ($\ell/D_o = 0$)

Tests of the canopy-alone configuration at Mach numbers of 2.3, 2.98, 3.5, and 3.71 indicated that, in all cases, the flow through the canopy was choked and spilling over as shown in parts of Figures 5 and 6. Two shock formations may be observed from these figures. One was usual and the other had a blister effect as shown in Figures 8 and 9. Enlargements of typical frames from the high-speed Schlieren movie film as seen in Figure 5 illustrate the variations in flow characteristics with Mach number which were seen during tests of the 20 percent porosity, canopy-alone configuration.

Parts (a) and (b) of Figure 5 in particular, exemplify the inconsistencies in flow pattern which were observed many times during this test program. The patterns seen were all obtained from the same test run of the 20 percent porosity canopy at a Mach number of 2.30. There was no change in the model or tunnel characteristics, and yet two distinct variations in the appearance of the shock pattern were evident. One explanation for the above considers that the shock pattern ahead of the canopy was alternating between the two patterns shown in parts (a) and (b) of Figure 5. It is believed that this

TABLE 3

RESULTS OF WIND TUNNEL TESTS IN UNITARY PLAN WIND TUNNEL AT THE LANGLEY RESEARCH CENTER, LANGLEY FIELD, VIRGINIA

Test Configuration	Mach No	Dynamic Pressure (psf)	Angle of Attack (degree)	Flow Characteristics
20% Porosity Canopy without Lines	2.30	200	0	Unsteady - changed from unsymmetrical bulging shock front to symmetrical shock front during test
	2.98	200	0	Steady
	3.50	200	0	Unsteady
	3.71	200	0	Steady
24% Porosity Canopy without Lines	3.00	200	0	Unsteady - Unsymmetrical bulging shock front
	3.04	200	0	Steady
	3.35	150	1.0	Unsteady - unsymmetrical bulging shock front
	3.60	125	0	Steady
	3.60	150	0	Unsteady - unsymmetrical bulging shock front
	3.70	140	0	Steady
	3.90	115	0	Steady
	3.90	115	4.0	Steady
20% Porosity Canopy plus Short Suspension Line System ($\ell/D_o = 1.0$)	1.57	200	0	Unsteady
	1.87	200	0	Unsteady
	2.16	200	0	Unsteady
	2.30	200	0	Unsteady
	2.98	200	0	Unsteady
	3.71	200	0	Unsteady
20% Porosity Canopy Plus Long Suspension Line System ($\ell/D_o = 2.0$)	3.20	100	0	Unsteady but improvement over previous configurations
	3.71	200	0	Unsteady but improvement over previous configurations

(a) M = 2.30 (Camera Speed - 2160 frames per second)
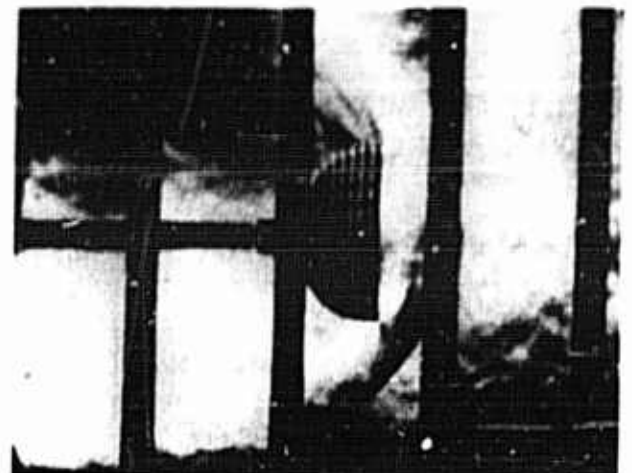
(b) M = 2.30 (Camera Speed - 2160 frames per second)

(c) M = ..98 (Camera Speed - 1440 frames per second)
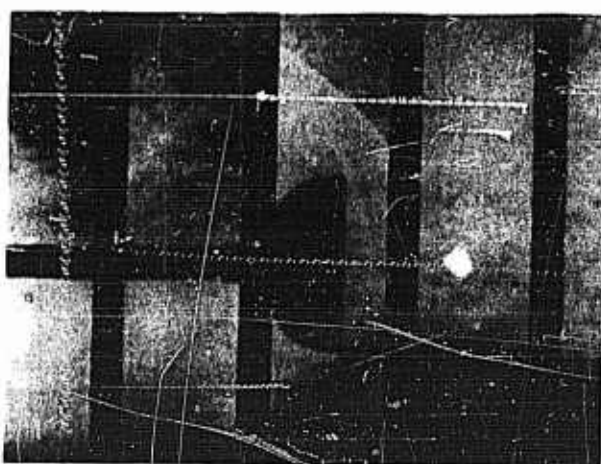
(d) M = 3.50 (Camera Speed - 1920 frames per second)
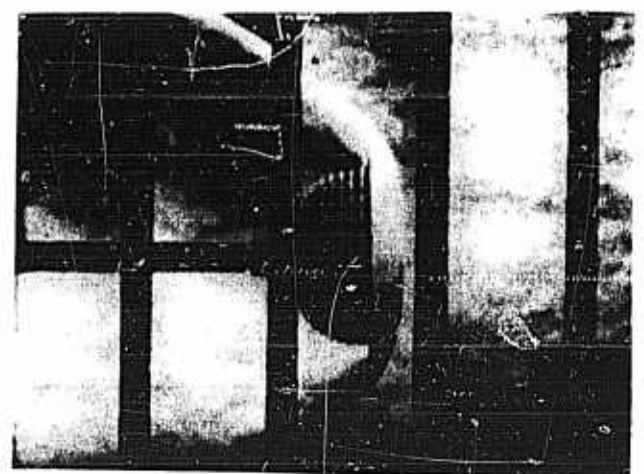
(e) M = 3.71 (Camera Speed - 1800 frames per second)

Figure 5. Shock Pattern Photographs - 20 Percent Porosity Canopy without Lines (q = 200 psf) (a = 0°)
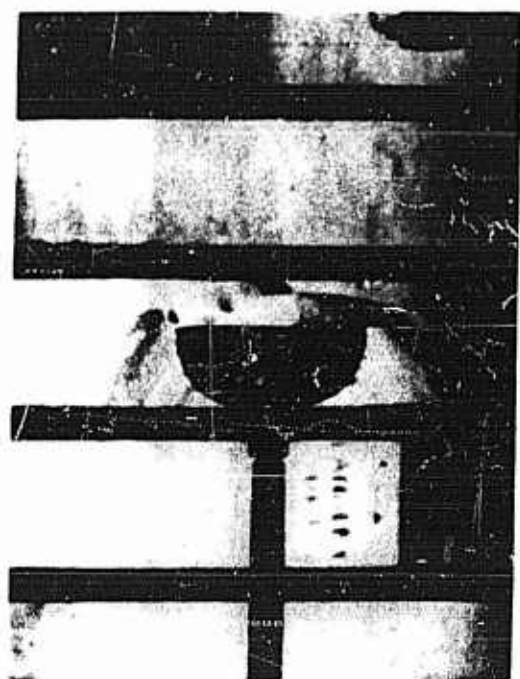
(a) M = 3.00 (q = 200 psf) (α = 0°)
(Camera Speed - 1680 frames per second)
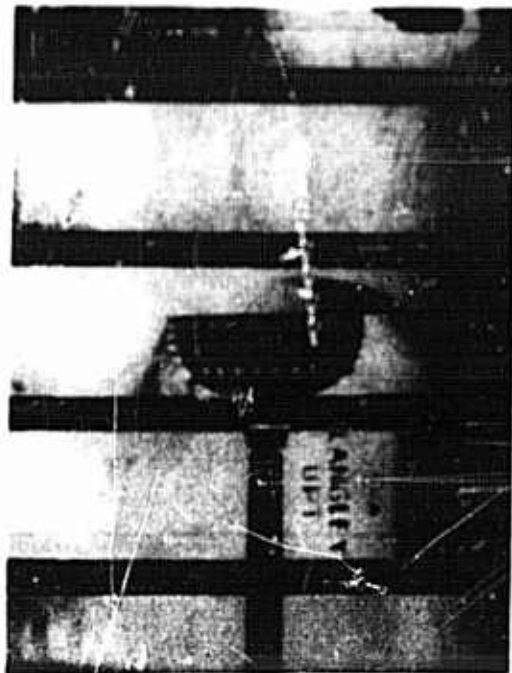
(b) M = 3.04 (q = 200 psf) (α = 0°)
(Camera Speed - 1680 frames per second)
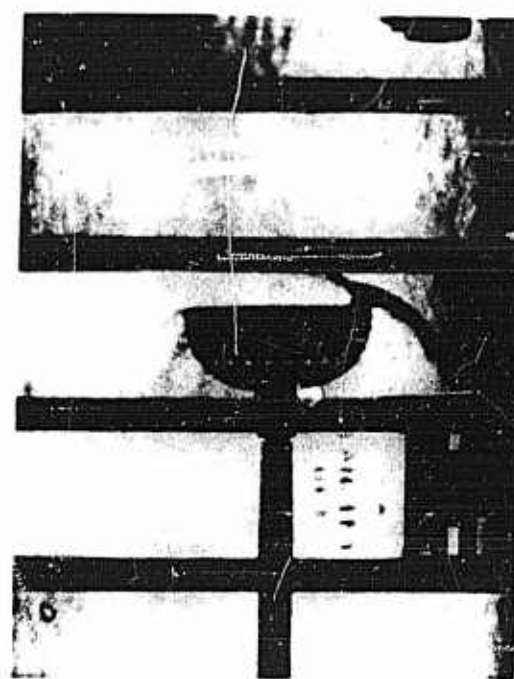
(c) M = 3.35 (q = 150 psf) (α = 5°)
(Camera Speed - 225 frames per second)
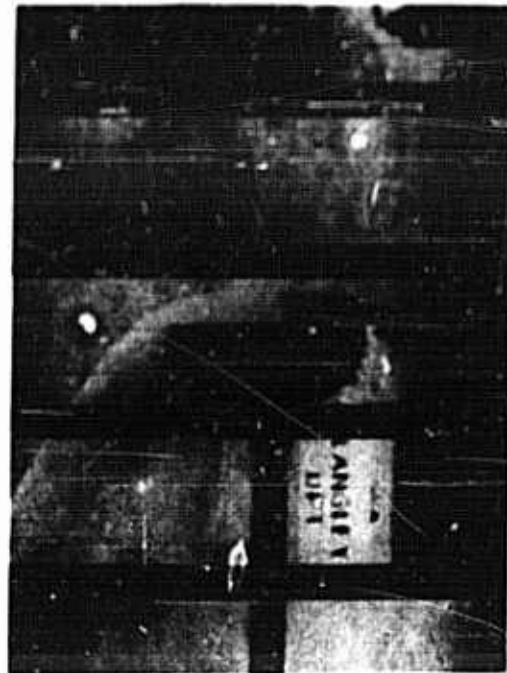
(d) M = 3.35 (q = 145 psf) (α = 5°)
(Camera Speed - 225 frames per second)

Figure 6 Shock Pattern Photograph - Model Performance Model
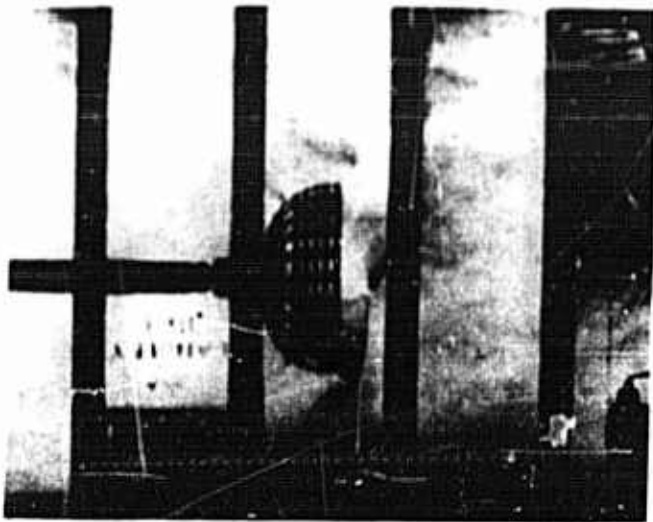
(e) M = 3.60 (q = 150 psf) (α = 0°)
(Camera Speed - 2280 frames
per second)
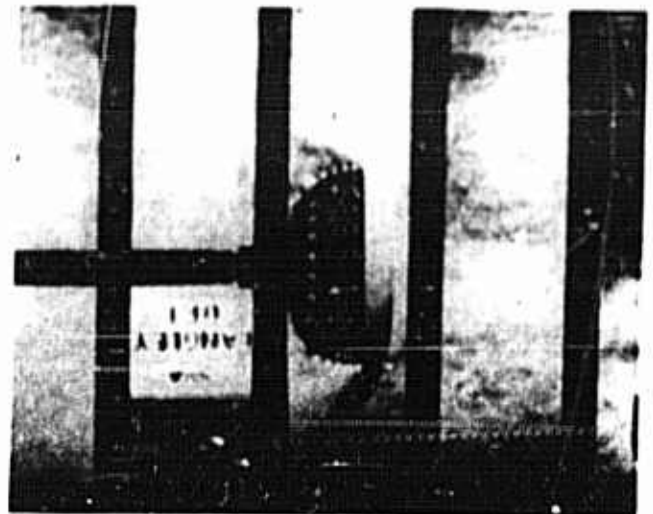
(f) M = 3.70 (q = 140 psf) (α = 0°)
(Camera Speed - 1800 frames
per second)
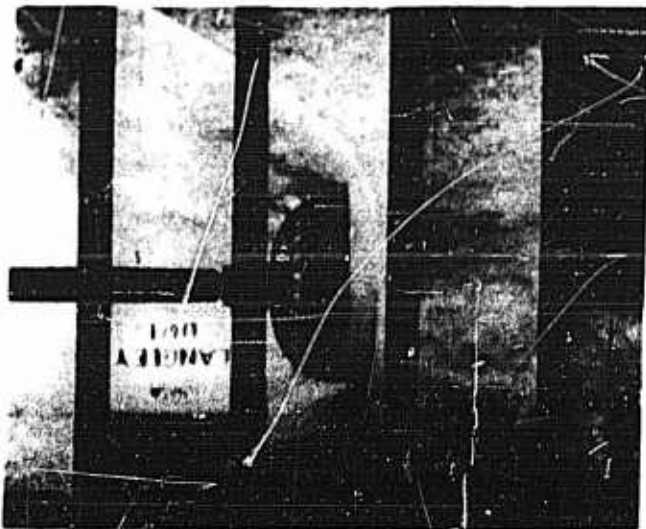
(g) M = 3.90 (q = 115 psf) (α = 0°)
(Camera Speed - 1860 frames
per second)
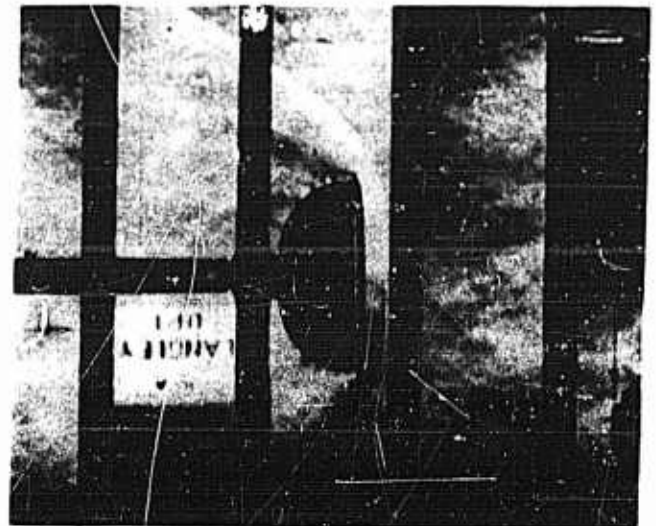
(h) M = 3.90 (q = 115 psf) (α = 4°
(Camera Speed - 1860 frames
per second)

Figure 6 (cont'd). Shock Pattern Photograph - 24 Percent Porosity Canopy without Lines

alternating shock pattern at a particular Mach number is the result of rotation of the bulging shock front (part (a) of Figure 5) about the canopy. Consequently, the high-speed movie camera, which only shows the two dimensions in its plane of projection, was taking pictures of a rotary action so that two distinct variations in pattern were visible on the film.

Most of the canopy-alone tests of the 20 percent porosity model exhibited rather violent rotary motion within the canopy. This motion was particularly noticeable during the test at a Mach number of 2.3. A great deal of canopy breathing or pulsing was also seen at this Mach number.

Shock pattern discontinuities and unstable flow characteristics, such as observed in these tests of the 20 percent porosity canopy-alone configuration, were also observed in preliminary wind tunnel tests of a 20 percent porosity, 2.5 inch inflated diameter, ribbon parachute canopy at a Mach number of 4.93 (Reference 8). The model of Reference 8 was constructed of stainless steel and was sting-mounted in the test section in a manner similar to that of the present tests. A comparison of the characteristics observed in the current program with those of Reference 8 indicates that the effects of scale or Reynolds number were insignificant.

In order to reduce the effects of choking, the number of slots in the canopy was increased. This was done by removing one complete ribbon (fifth up from the skirt) and symmetrical portions of the eighth ribbon. Tunnel time limitations prevented the complete removal of this eighth ribbon. Figure 13 shows this modified canopy as well as the original 20 percent porosity canopy as it was prior to modification. Differences between the gore layouts of the modified and unmodified canopies can be seen in Figure 12.

The additional open area created by the above increased the geometric porosity about 4 percent to give a total porosity of approximately 24 percent. This increase in porosity was apparently not significant enough to cause a marked improvement in the flow characteristics but it tended to stop the apparent internal rotary motion which was witnessed for the 20 percent porosity canopy.

The above indicates that the amount of porosity required to achieve stable flow conditions could not be achieved without an extensive test program. Some theoretical knowledge of the porosity required can be obtained, however, by assuming sonic velocity or Mach 1.0 flow exists in the slots behind the normal shock at the

canopy skirt and calculating the critical area ratios at which choking occurs. The method and sample calculations for determining the porosity required to yield a zero spillover condition are shown in Appendix V. A curve of this calculated porosity as a function of Mach number is shown in Figure 19.

The 24 percent porosity canopy-alone configuration was tested at Mach numbers of 3.0, 3.04, 3.35, 3.6, 3.7, and 3.9. The photographs shown in Figure 6 indicate that the variations in shock pattern which were observed were completely haphazard and impossible to correlate. However, once a particular flow condition was established, it remained so for a period of time and was completely independent of Mach number, dynamic pressure, and even angle of attack. It is suspected however that, in the case of a flexible canopy, interaction effects would cause fluctuations of the established flow condition.

3. Canopy Plus Short Suspension Line System (ℓ/D_o = 1.0)

Prior to modification from 20 percent to 24 percent porosity, the canopy was tested in conjunction with both ℓ/D_o = 1.0 and ℓ/D_o = 2.0 suspension line systems. Tests on the canopy plus short lines (ℓ/D = 1.0) were conducted at six Mach numbers varying from 1.57 to 3.91. Figure 7, which is composed of enlargements of typical frames from high-speed Schlieren movies, indicates considerable whipping motion of both the bow wave and normal shock.

There was little noticeable difference in the performance of the model at Mach numbers of 1.57, 1.87, and 2.16. The flow was generally unsteady at all of these Mach numbers. Since a Mach number of 1.57 is the lowest which can be obtained in the Unitary Tunnel at Langley, it was impossible to determine any effects at Mach numbers less than 1.57. Parts (a), (b) and (c) of Figure 7 show the variations in the appearance of the bow shock at Mach numbers of 1.57, 1.87, and 2.16, respectively. Typical three-frame sequences as shown in the figure give some indication of the fluctuation and distortion tendencies which were observed during this series of tests. Fluctuation or distortion of the bow wave during the M = 1.57 to 2.16 series of tests was occurring at a rate of approximately 350 cps. This rapid distortion action of the bow wave was apparently caused by the tendency of the normal or secondary shock to detach from the skirt of the canopy and move upstream, thus distorting the bow wave.

A 1 degree angle of attack at a Mach number of 2.16 had little effect on the unsteady flow characteristics of the model.

(a) Sequence of Three Consecutive Frames Showing Variation in Appearance of
Bow Shock at M = 1.57 (α = 0°) (Camera Speed - 1560 frames per second)
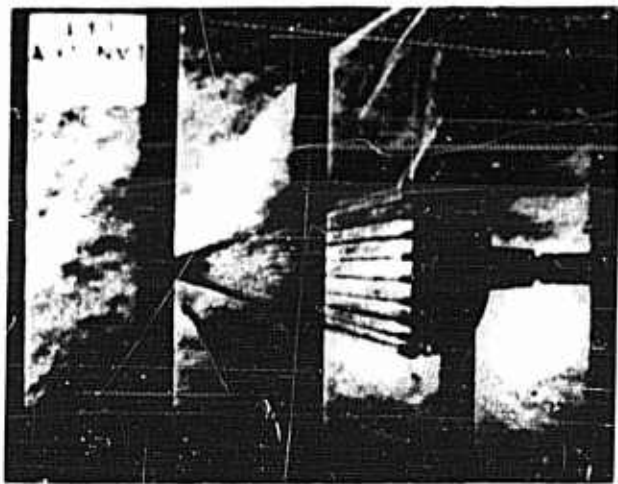
(a) Cont'd)

(b) M = 1.87 (α = 0°)
(Camera Speed - 1920 frames per second

(b) Cont'd.
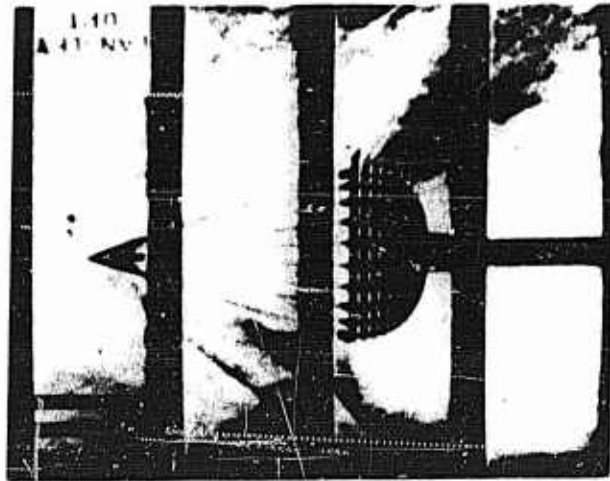
(b) Cont'd.

Figure 7. Shock Pattern Photographs - 20 Percent Porosity Canopy Plus
Short Suspension Line System (l/D_o = 1.0) (q = 200 psf)

(c) Sequence of Three Consecutive Frames Showing Variation in Appearance of
Bow Shock at M = 2.16 (a = 0°) (Camera Speed - 1500 frames per second)
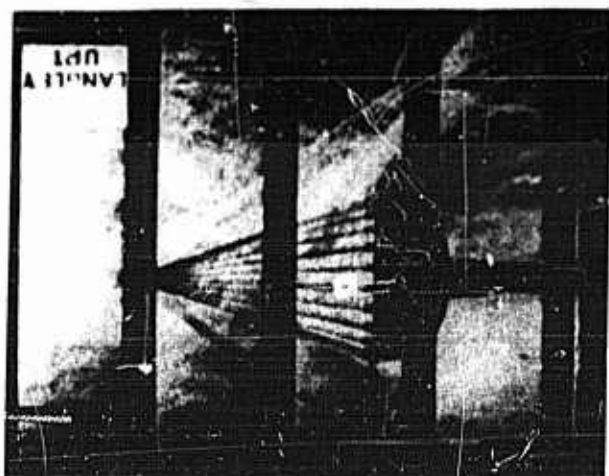
(c) Cont'd.
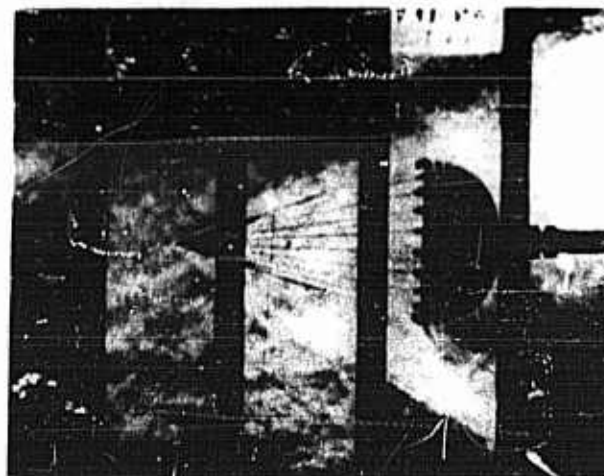
(d) M = 2.30 (a = 0°)
(Camera Speed - 480 frames per second)
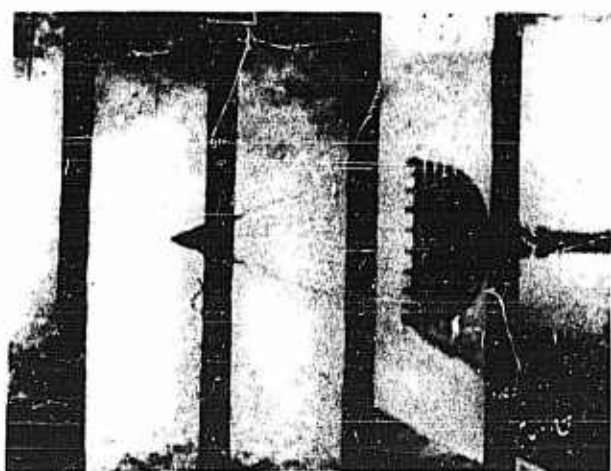
(e) M = 2.98 (a = 0°)
(Camera Speed - 960 frames per second)
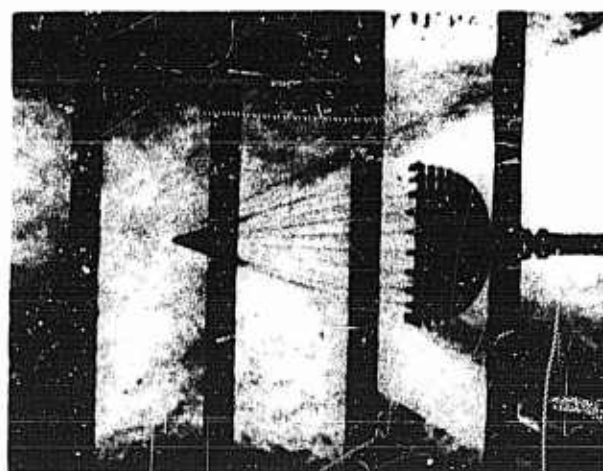
(f) M = 3.71 (a = 0°)
(Camera Speed - 480 frames per second)

Figure 7 (cont'd). Shock Pattern Photographs - 20 Percent Porosity Canopy
Plus Short Suspension Line System ($\ell/D_o = 1.0$)
(q = 200 psf)

Similar action to that discussed above was indicated in tests of
the model at Mach numbers of 2.30, 2.98, and 3.71. Parts (d), (e)
and (f) of Figure 7 are typical of the shock patterns at these Mach
numbers.

The influence of the shock wave fluctuation and distortion ten-
dencies, as seen for this configuration (Figure 7) is considered in the
explanatory discussion of the reduced drag and inflation characteris-
tics given in Appendix IV.

4.   Canopy Plus Long Suspension Line System (ℓ/D_o = 2.0)

Tests of this configuration were conducted at Mach numbers of
2.98, 3.20, and 3.71. Photographs of the shock patterns at Mach
numbers of 3.20 and 3.71 are given in parts (a) and (b), respectively,
of Figure 8. It may be seen from this figure that flow conditions were
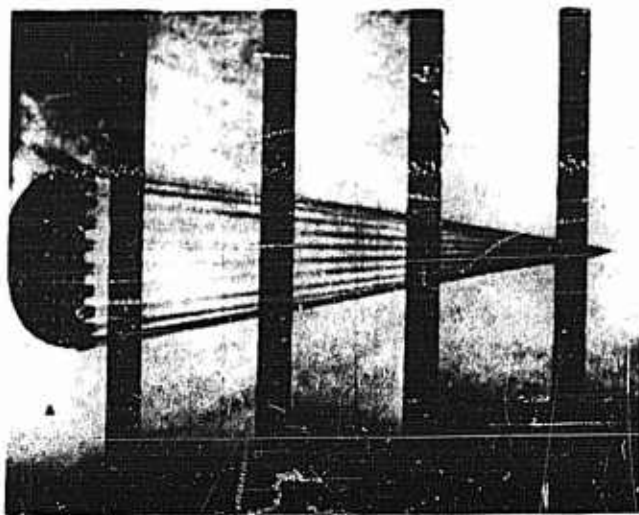
(a) M = 3.20 (q = 100 psf)
     (Camera Speed - 2160 frames per second)
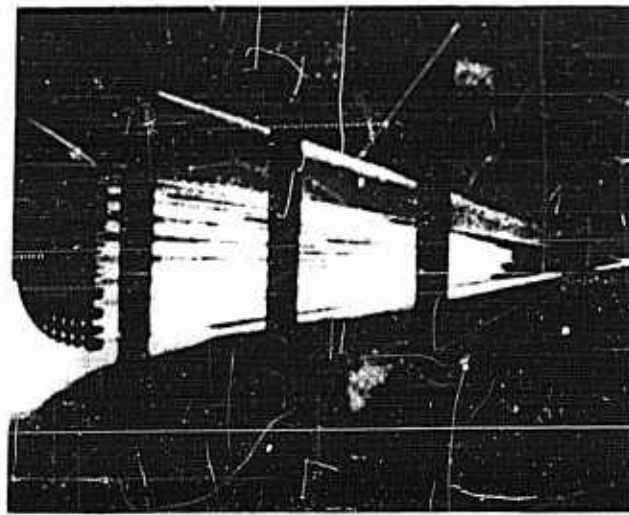
(b) M = 3.71 (q = 200 psf)
     (Camera Speed - 480 frames per second)

Figure 8   Shock Pattern Photographs - 20 Percent Porosity Canopy Plus
            Long Suspension Line System (ℓ/D_o = 2.0) (a = 0°)

somewhat improved over those occurring for previously tested con-
figurations. The fluctuation of the bow shock was relatively insigni-
ficant at Mach numbers of 3.20 and 3.71. However, at M = 3.20, the
normal shock tended to detach from the canopy skirt, move upstream
and back and then reattach. No such normal shock action was noted
at the 3.71 Mach number since the normal shock seemed to remain
attached to the skirt of the canopy. Considerable suspension line
bending was noted for the M = 3.20 case, but not for the higher Mach
number of 3.71.

SECTION IV

CONCLUSIONS

The preceding discussion indicates that the problems or factors influencing the performance of parachutes at supersonic speeds are manifold. Some of the more important of these problems are discussed in the following paragraphs. In addition, some general remarks regarding considerations for future test programs are included.

It may be concluded from the Lewis wind tunnel program that the following factors have been responsible for the results achieved there:

(1) Violent breathing or pulsing

(2) Reduced inflation and drag associated with (1) above

(3) Interaction effects due to flow characteristics and canopy flexibility

(4) Oscillation resulting in failure of materials at relatively low loading conditions. Material failure was due to fatigue rather than loading.

Obviously then, in the development of a parachute configuration suitable for supersonic operation, effort must be directed toward resolution of the problems as given above. In this regard the logical approach to be pursued as a result of the Lewis tests was the one taken in which the effects of flexibility were canceled by the use of rigid models. This was the recommendation of these Laboratories and the main purpose for instituting the Langley program.

The results of tests in the wind tunnel at Langley indicated that variations in the shock patterns were completely haphazard and relatively independent of Mach number, dynamic pressure, and angle of attack. In addition, shock pattern discontinuities and unstable flow characteristics at particular Mach numbers were observed for most of the test configurations. Information reported in Reference 7 relative to the flow characteristics of a 20 percent porosity 2.5 inch canopy-alone configuration tends to substantiate the occurrence of these discontinuities and unstable flow characteristics. Further comparison of the characteristics of Reference 7 with the current program indicated no effects of Reynolds number.

Some knowledge of the porosity required to reduce the severe choking conditions which were in evidence was realized by assuming Mach 1.0 flow in the canopy slots and calculating the critical area ratios which will give zero spillover as illustrated in Appendix IV. The results of these calculations are shown in Figure 19 as a function of Mach number. The required porosity varies with Mach number from 41 percent at Mach 1.5 to 29.5 percent at Mach 4.0.

It should be noted that at all Mach numbers the calculated porosities are higher than those normally used in conventional parachute designs and also higher than those used in the parachutes and models tested to date. Hence, no actual test data are presently available and therefore, a future test program should be directed towards the examination of parachutes with very high geometric porosities. In order to obtain an adequate spread in the data the best approach would be to construct a series of models with porosities ranging from 25 to 45 percent.

In order to determine the characteristics of the various models being tested so that the behavior of actual parachutes can be predicted, it will be necessary to measure pressures at various point inside the canopy. Also, since full inflation of a parachute results in tensile stresses in the skirt ribbons, strain gages should be employed to determine the tension in the skirt. This information would aid in the determination of a parachute configuration which would give a fully inflated condition.

Since the results of this program have indicated the need for further development work, future wind tunnel test programs (carried on under Contract No. AF 33(616)-5507) will employ test models with which the effects of higher porosity on flow stabilization will be studied. In addition, the effects of vents and their size, slot orientation, clustered parachutes, other parachute types, etc., will be considered in future test programs.

REFERENCES

1. Downing, J. R., et al., Recovery Systems for Missiles and Target Aircraft, Part III - High Subsonic and Transonic Trackborne Parachute Tests, WADC Technical Report 5853 Cook Research Laboratories, A Division of Cook Electric Company, Chicago, Illinois, December 1956

2. Wiant, H. W. and Fredette, R. O., A Study of High Drag Configurations as First Stage Decelerators, WADC Technical Note 56-320, Cook Research Laboratories, A Division of Cook Electric Company, Chicago, Illinois, July 1956

3. Moeckel, W. E., Flow Separation Ahead of Blunt Bodies at Supersonic Speeds, NACA TN 2318, July 1951

4. Stalder, J. R. and Nelsen, H. V., Heat Transfer from a Hemisphere-Cylinder Equipped with Flow Separation Spikes, NACA TN 3287, September 1954

5. Jones, J. J., Experimental Drag Coefficients of Round Noses with Conical Windshields at Mach Number 2.72, NACA RM L55E10, 28 June 1955 (CONFIDENTIAL)

6. Roschke, E. J. and Piddington, M. J., Drag and Dispersion of Banded Spheres with and without Stings, BRL Memorandum Report No. 995, Ballistics Research Laboratories, Aberdeen Proving Ground, Maryland, April 1956

7. Anonymous, X-7A Supersonic Ramjet Test Vehicle Parachute Recovery System, Section I - Pretest and Test Program, Section II - Recovery Systems, WADC Technical Report 55-162, Lockheed Aircraft Corporation, Missile Systems Division, Van Nuys, California, June 1955 (CONFIDENTIAL)

8. Heinrich, H. G., and et al., Theoretical Parachute Investigations, Progress Report No. 2, Department of Aeronautical Engineering, No. 8182, Department of Aeronautical Engineering, University of Minnesota, Minneapolis, Minnesota, 1 September 1957

9. Topping A. D., Marketos, J. D., and Costakos, N. C., A Study of Canopy Shapes and Stresses for Parachutes in Steady Descent, WADC Technical Report 55-294, Goodyear Aircraft Corporation, Akron, Ohio, October 1955

10. Timoshenko, S., *Advanced Strength of Materials*, Vol. II, McGraw-Hill Book Company, Inc., New York, N. Y.

11. Ames Research Staff, *Equations, Tables and Charts for Compressible Flow*, NACA Report 1135, 1953

APPENDIX I

FABRIC PARACHUTE DESIGN

A   Introduction

Three guide surface ribless parachutes and 11 FIST ribbon parachutes were designed for high-speed wind tunnel tests. The objectives were (1) to determine and bracket the parameters which yield stability, and (2) establish the strength of the materials used.

Past experience in the design of high-speed parachutes played a major role in selecting proper materials which could withstand pressure conditions in supersonic flow.

The range of variables and design procedure are outlined herein for both types of fabric canopies under study as high Mach drag devices. The basic configurations were altered as the test program progressed.

1   Guide Surface Ribless Parachutes

The three guide surface ribless (G.S.R.) parachutes had a 1 percent vent area with 0, 10, and 20 percent slots, respectively. All dimensions of the individual gores were a function of diameter which varied from 2.67 feet to 3.25 feet. The suspension lines were one diameter in length from the skirt to the confluence point.

A more detailed list of materials and gore geometry is given in Table 4. A typical layout of the roof panel and guide surface panel is illustrated in Figure 9.

2   FIST Ribbon Parachutes

Perhaps the most important parameter in the design of FIST ribbon parachutes is the geometric porosity. Therefore, accuracy was emphasized when determining the open area within the boundaries of the canopy.
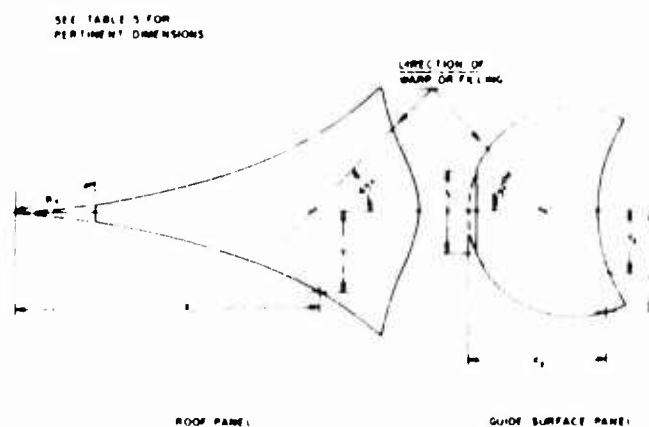
Figure 9. Panel Layout - Guide Surface Ribless Parachute

TABLE 4

GEOMETRY AND MATERIALS, GUIDE SURFACE RIBLESS PARACHUTES

Parachute No. 220

Panel Material	~ 4.75 oz/yd	300 lb/in.
Suspension Lines	~ 3-4	2250 lb
Vent Reinforcing	~ 1 in.	3030 lb
Skirt Reinforcing	~ 1 in.	1000 lb

D_{max} = 2.67 feet

n = 8 gores

Panel Coordinates are in inches

X_1	1.60	2.40	3.20	4.81	6.41	8.01	9.61	11.21	12.82	14.41	15.21	15.61	16.02
Y_1	0.85	1.25	1.65	2.47	3.28	4.10	4.90	5.89	7.54	9.5	3.97	2.52	0.00
X_2	0.37	0.74	1.11	1.47	2.21	2.95	3.68	4.42	5.16	5.89	6.76	7.00	7.37
Y_2	2.04	2.82	3.20	3.57	3.98	4.19	4.31	4.25	4.15	4.00	3.96	3.91	3.81
Y_3	-	-	-	-	-	-	-	-	-	-	0.0	2.14	-

Slot, S, = 3.20 in.

Parachute Nos. 496 and 510

Panel Material	~ 4.75 oz/yd²	3C0 lb/in.
Suspension Lines	~ 1 in.	3000 lb
Vent Reinforcing	~ 1 in.	3000 lb
Skirt Reinforcing	~ 3/4 in.	2250 lb

D_{max} = 3.25 feet

n = 16 gores

Panel Coordinates are in inches

X_1	1.95	2.92	3.90	5.85	7.80	9.75	11.70	13.65	15.60	17.30	17.56	18.52	19.00	19.50
Y_1	0.59	0.89	1.19	1.80	2.42	3.09	3.93	5.00	6.76	10.75	9.72	4.84	3.08	0.0
X_2	0.45	0.90	1.35	1.80	2.69	3.59	4.49	5.38	6.28	7.18	8.07	8.46	8.52	8.96
Y_2	1.73	2.49	2.94	3.28	3.68	3.86	3.92	3.86	3.71	3.47	3.36	3.36	3.36	3.21
Y_3	-	-	-	-	-	-	-	-	-	-	0.0	0.76	0.0	3.21

S = 0.0 for Parachute No. 496   S = 7.8 in. for Parachute No. 510

The canopies were constructed with radial, horizontal, and vertical ribbons all of which were considered impervious and assumed to have zero material porosity

Two types of FIST ribbon parachutes were designed and tested. The regular canopy had horizontal ribbons equally spaced from vent to skirt and was denoted by a single porosity value. A typical gore layout is shown in Figure 10. In the modified canopy two values of equal ribbon spacing existed. The one spacing applied to the crown region from
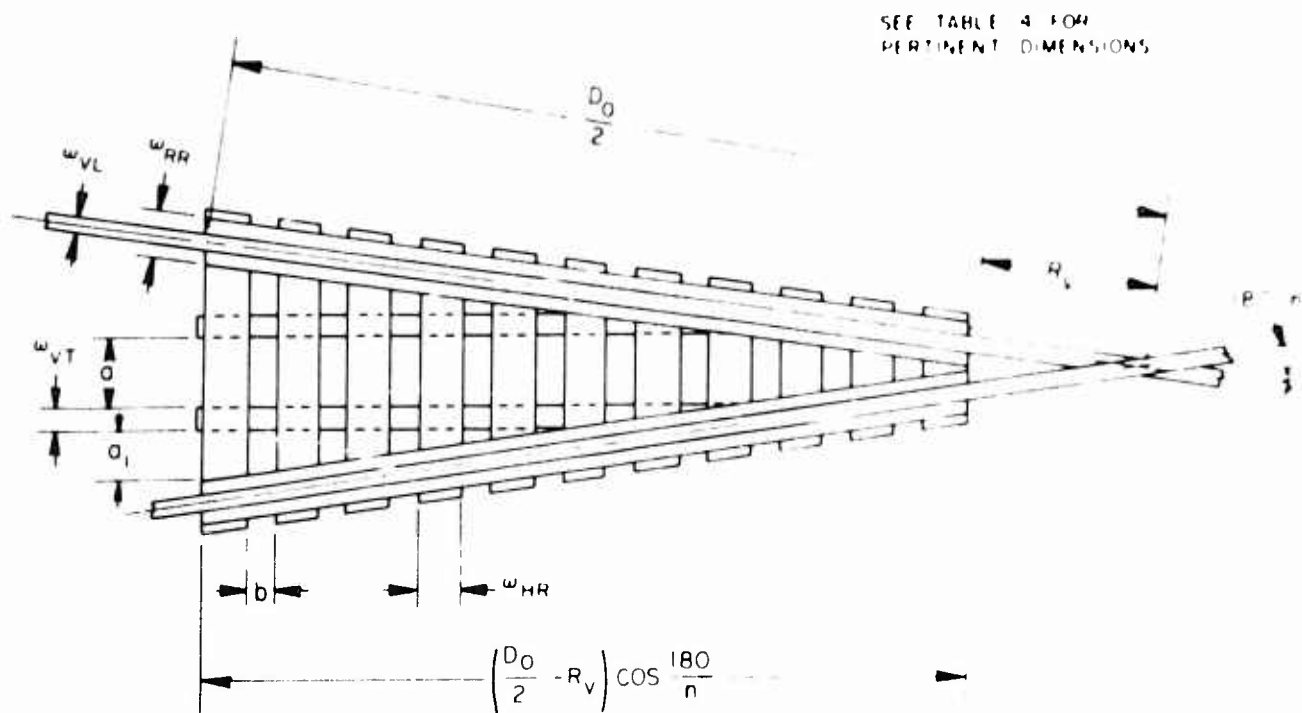
Figure 10. Typical Gore Layout - FIST Ribbon Parachute

the vent radius to approximately two-thirds the diameter. The second spacing applied to the skirt area from two-thirds the diameter to the base of the gore. The porosity of the skirt and crown were calculated by treating the whole parachute as two individual canopies. A typical modified gore layout is illustrated in Figure 11

The geometric porosity, number of gores, flat diameter, materials, etc., are listed in Table 5 for all FIST ribbon parachutes designed for the test program.

Although the following example applies to the 24 gore, 3.66 foot diameter FIST ribbon parachute, the same method and formulas were used to estimate the geometric porosity of all the FIST canopies.
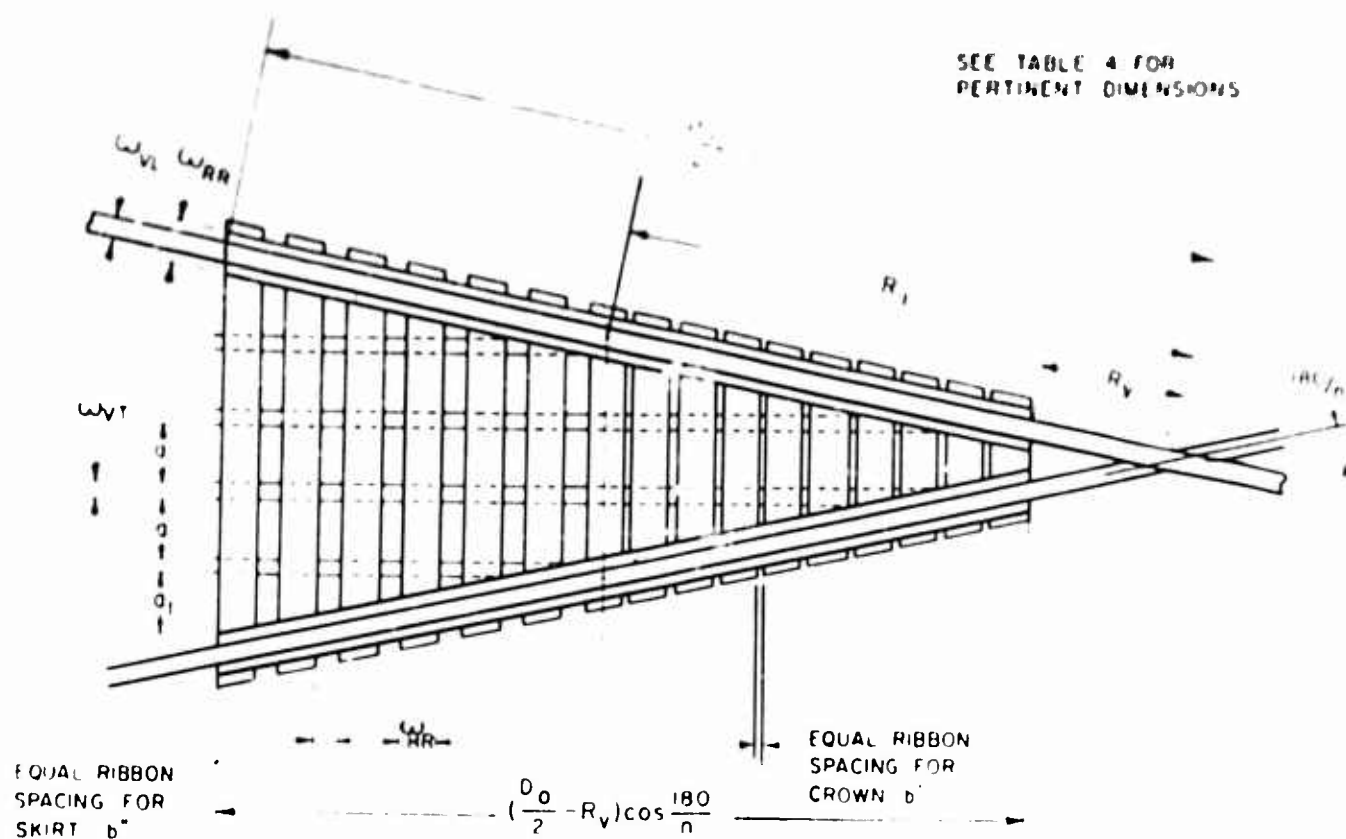
Figure 11. Typical Gore Layout - FIST Ribbon Parachute

Initially, the materials were selected, the number of gores were established, and the diameter was tentatively fixed. The desired geometric porosity, λ_g, was 19 percent of the total flat area.

The flat area of the canopy is

$$S_o = \frac{nD_o^2}{4} \left(\sin \frac{180}{n} \right) \left(\cos \frac{180}{n} \right) = 1502 \ in^2$$

where

D_o = flat diameter of canopy = 3.66 ft

n = number of gores = 24

As a general rule the open area at the vent, s, is 1 percent of the flat area. Or

$$s = 0.01 \ S_o = 15.02 \ in^2$$

TABLE 5

GEOMETRY AND MATERIALS FIST RIBBON PARACHUTES

Parachute Number	469	472	473	495	505	506	505	508 511-14	490	490
Flat Diameter, D_o ~ feet	4.25	2.14	4.11	4.30	4.00	3.92	3.66	3.66	4.00	3.64
Geometric Porosity, λ_g ~ percent	19.3	26.3	11.0	23.0	29.4	5.6	10.12	19.2	11/21 (1)	11/21 (1)
Number of Gores, n	8	8	8	16	16	16	24	24	8	16
Vent Radius, R_V ~ inches	4.0	2.10	3.89	3.85	3.71	3.66	4.14	4.14	1.94/15.8 (2)	1.94/15.8 (2)
Gore Dimension, a_1 ~ inches	2.00	3.04	4.24	1.64	1.17	1.07	1.05	1.05	4.04	4.04
Horizontal Ribbon Width, W_{HR} ~ in.	2.0	1.5	2.0	1.0	1.0	1.0	1.0	1.0	2.0	2.0
Horizontal Ribbon Strength ~ lb	1700	1500	1700	1000	600	600	600	600	1700	1700
Horizontal Ribbon Number, m	7	4	8	14	11	18		11	7	15
Horizontal Ribbon Spacing, b ~ in.	0.984	1.29	0.46	0.578	0.89	0.084		0.648	0.515/1.25	0.167/0.444
Vertical Ribbon Width, W_{VT} ~ in.	9/16 2 ply	9/16 2 ply	9/16 2 ply	3/8 2 ply	1.0 folded to 3/8 in.	1.0 folded to 3/8 in.	9/16 2 ply	9/16 2 ply	9/16 2 ply	1.0 folded
Vertical Ribbon Strength ~ lb	500	500	500	200	525	525	500	500	500	1000 core
Vertical Ribbon Number, p (per gore)	6	2	4	4	4	4	2	2	4	14
Vertical Ribbon Spacing a ~ in.	2.0	2.0	2.0	1.41	1.5	1.5	1.5	1.5	2.0	
Radial Ribbon Width, W_{RR} ~ in	2.0 2 ply	1.0 2 ply	2.0 2 ply	1.0 2 ply	1.0 2 ply	1.0 2 ply	1.0 2 ply	1.0 2 ply	2.0 2 ply	1.0 2 ply
Radial Ribbon Strength ~ lb	1700	1000	1700	1000	600	600	600	600	1700	600
Vent Reinforcing Width, W_{VP} ~ in	1.0	1.0	1.0	1.0	1.0	1.0	1.0	1.0	1.0	1.0
Vent Reinforcing Strength ~ lb	6000	3000	6000	6000	6000	6000	6000	6000	6000	6000
Intermediate Rein Width, W_{RB} ~ in					1.0	1.0				
Intermediate Rein Strength ~ lb					600	600				
On Rbn No					8, 9 & 16	14, 15 16 & 17				
Skirt Reinforcing Width W_{SR} ~ in	1.0	1.5	1.75	1.0	1.0	1.0	1.0	1.0		
Skirt Reinforcing Strength ~ lb	6000	1500	6000	3000	3000	3000	3000	3000	3000	3000
Suspension Line Width, W_{VL} ~ in	1.0	0.1b		1.0		1.0	1.0	1.0	1.0	1.0
Suspension Line Strength ~ lb	6000	1500	6000	6000		6000	3000	3000	6000	6000

(1) λ of Crown / λ of Skirt
(2) Vent Radius R_V, R, as indicated in Figure...
(3) W_{HR} of Crown / W_{HR} dia...
(4) Strength / Crown Strength...

The vent radius, R_V, required to yield the 15.02 in² of open area is

$$R_V = \frac{0.5 \, W_{VL}}{\sin \frac{180}{n} \, \cos \frac{180}{n}} + \sqrt{\frac{0.01 \, S_o}{n \, (\sin \frac{180}{n}) \, (\cos \frac{180}{n})}} = 4.13 \text{ in.}$$

In this case, W_{VL} is the width of the continuous suspension line crossing the vent.

The spacing between horizontal ribbons, b_1, is approximated in terms of desired geometric porosity, λ_g, horizontal ribbon width, W_{HR}, and vertical ribbon width, W_{VT}.

$$b_1 = \frac{W_{HR}}{\dfrac{100a}{(W_{VT} + a) \, (\lambda_g + k)} - 1} = 0.600$$

a = spacing between vertical ribbons = 1.5 in.

k = scale factor for small canopies = 8.3

The number, m, of horizontal ribbons which will fit in the space between the vent and skirt is

$$m \cong \frac{(\dfrac{D_o}{2} - R_V) \cos \dfrac{180}{n} + b_1}{W_{HR} + b_1} \cong 11 \text{ (nearest whole integer)}$$

The actual equal spacing of the 11 horizontal ribbons is

$$b = \frac{1}{m-1} \left[(\frac{D_o}{2} - R_V) \cos \frac{180}{n} - m \, W_{HR} \right] = 0.668 \text{ in.}$$

The area sum of geometric openings, A_{OH}, between horizontal ribbons (neglecting the area blocked by vertical tapes) is

$$A_{OH} = bn \left[m - 1 \right] \left[(R_V + \frac{D_0}{2}) \sin \frac{180}{n} - \frac{W_{Rn}}{\cos \frac{180}{n}} \right] \quad 385 \text{ in}^2$$

The open area blocked by vertical tapes, A_{BV}, is the product of the horizontal ribbon spacing, b, and the vertical tape width, W_{VT}, times the number of blocking elements, g.

$$A_{BV} = gb \, W_{VT} = 111.0 \text{ in}^2$$

Finally, the geometric porosity is

$$\lambda_g = (s + A_{OH} - A_{BV}) \frac{100}{S_0} = 19.2 \text{ percent}$$

The porosity may be refined to any exact value by adjusting the diameter and ribbon spacing. In some cases the width of the radial ribbon was reduced yielding as much as 8 percent more open area.

APPENDIX II

RIGID PARACHUTE MODEL DESIGN

The model was designed to simulate a parachute with an inflated FIST Ribbon type canopy. Every attempt was made to achieve a realistic replica with no deviations except where strength of fabrication requirements necessitated it.

Originally it was specified that the canopy of the model be designed so that the porosity could be varied automatically from controls located outside the test section of the wind tunnel. However, aerodynamic limitations on the geometry of any system that might be used to accomplish this, so complicated the design that this feature was eliminated. It was then decided to pattern the canopy after a 3.66 foot diameter, FIST ribbon canopy composed of twenty-four 1 inch radial ribbons and eleven 1 inch horizontal ribbons spaced to provide a porosity of 20 percent. A typical gore layout is shown in Figure 12.

The canopy was made from a stainless steel spinning in which a pattern of rectangular slots was cut to form the ribbons (see Figure 13). The vertical ribbons, normally found on all FIST type canopies, were omitted to facilitate fabrication. The vent area of apex of the canopy was left solid so that the canopy could be attached to the wind tunnel sting. The contour of the canopy was that formed by the gore centerlines of a solid, flat, circular type parachute canopy. The construction details, shown in Figure 14, were based on information obtained from Reference 9.

Three separate sets of 1/8 inch diameter suspension lines were designed for the model. Each set of lines was of a different length but was otherwise identical in every detail. This was done to permit an investigation of the effects of suspension line length on the aerodynamics of the model. Particular care was
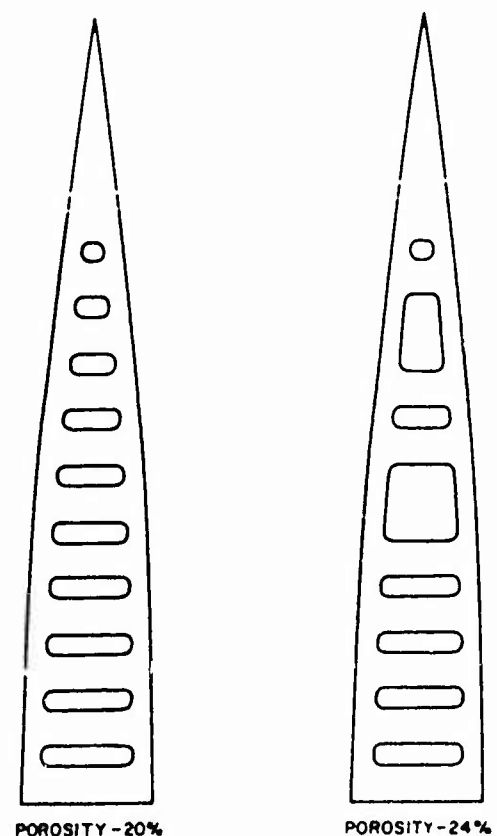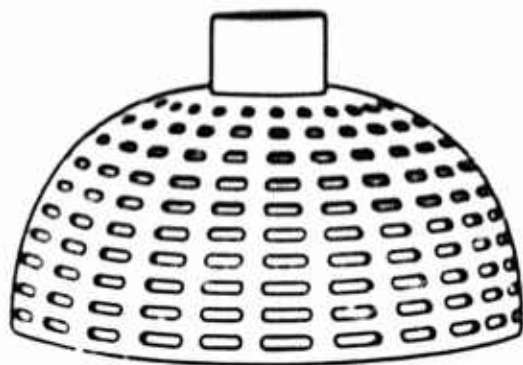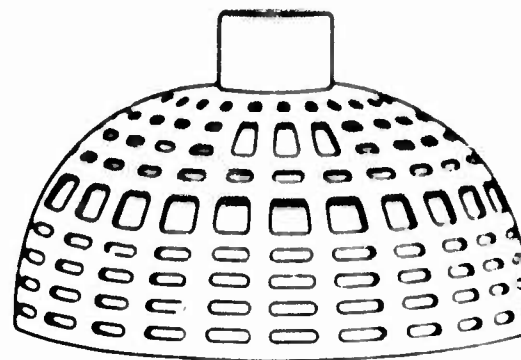

POROSITY - 20%   POROSITY - 24%

Figure 12. Typical Canopy Gore Layouts Showing Details of the Slots

BEFORE MODIFICATION
POROSITY-20%

AFTER MODIFICATION
POROSITY 24%

Figure 13. Canopy Configurations Before and After Modification

taken to design suspension line attachments that were aerodynamically clean and would permit the lines to be easily attached to the canopy. The attachment at the confluence point of the lines also contained a feature which would permit the geometry of its apex to be changed. While the clevis attachment (refer to Figure 15), used at the canopy end of the lines, was not quite satisfactory from an aerodynamic standpoint, its size was dictated by strength requirements.

The model was built to a scale of 1 to 3.66. This scale was used since it provided the largest model that could be conveniently accommodated in the high-speed test section of the Langley wind tunnel.
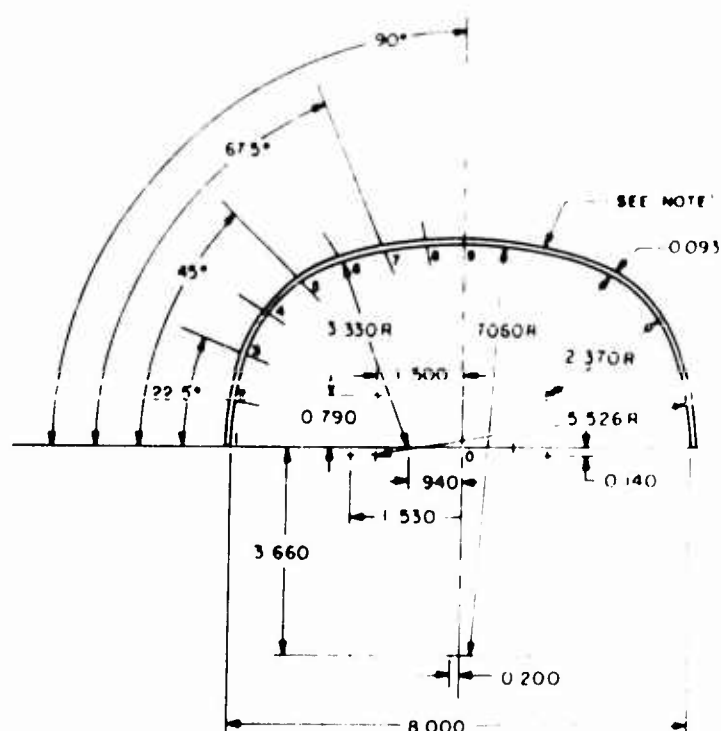
NOTE   CANOPY CONTOUR FORMED BY THE GORE CENTERLINES OF A FULLY INFLATED FLAT TYPE T-7 CANOPY (REFERENCE 9)

RADIAL LEGEND		
FROM	TO	LENGTH (IN.)
0	1	4 000
0	2	4 000
0	3	4 045
0	4	4 045
0	5	3 925
0	6	3 770
0	7	3 595
0	8	3 389
0	9	3 395

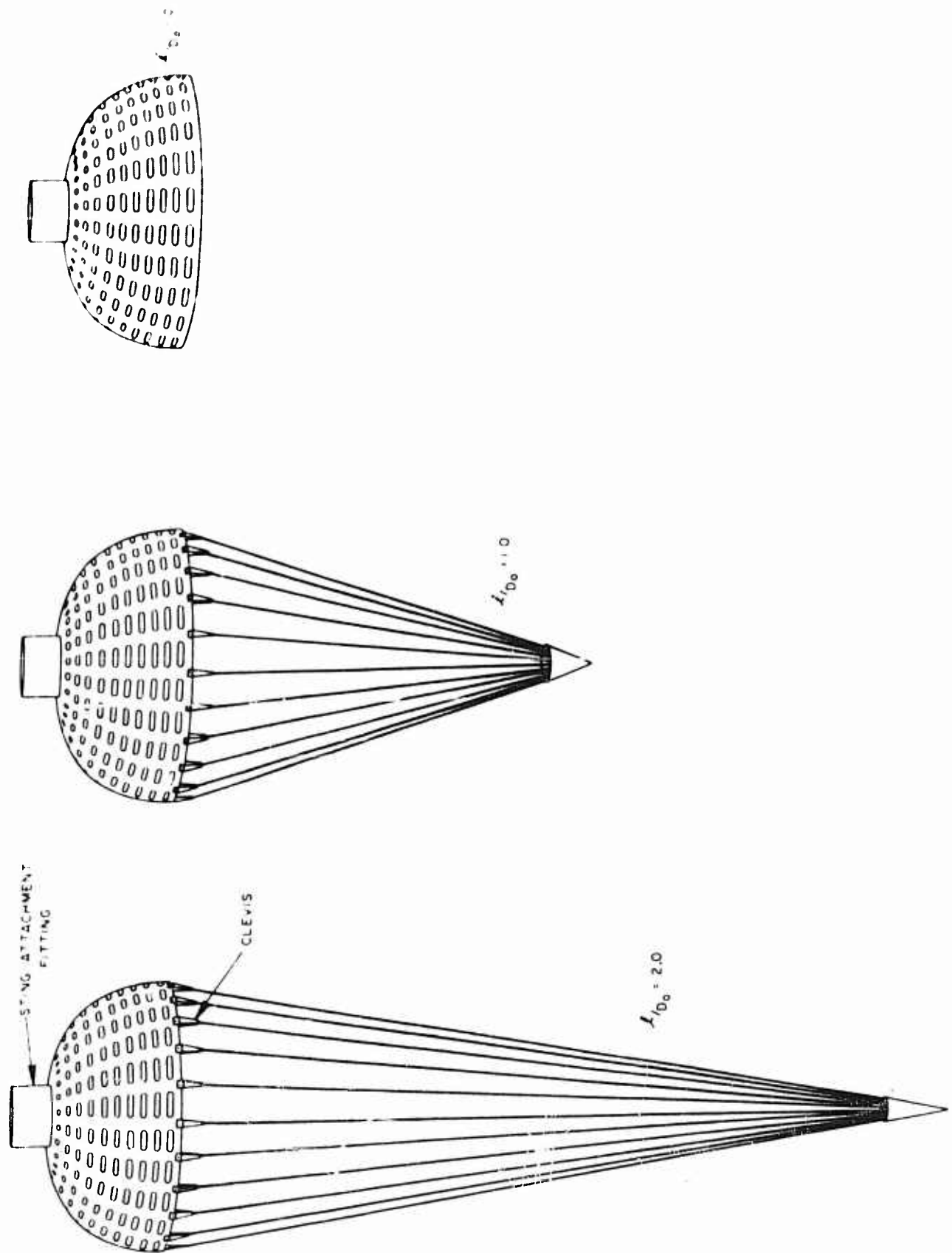Figure 14.   Dimensional Details of the Canopy Contour

Figure 15. Wind Tunnel Test Configurations Showing Suspension Line Systems Tested

APPENDIX III

STRESS ANALYSIS OF AN 8 INCH DIAMETER RIGID PARACHUTE MODEL

This analysis covers the strength of a rigid parachute model under room temperature conditions and a dynamic pressure of 100 lb/ft^2. While the entire structure of the model has been thoroughly examined, this analysis reports only on the more critical components.

It is believed that the methods used in this analysis are obvious with the possible exception of the calculation of the discontinuity stresses in the canopy. A complete discussion of the method used to calculate these stresses can be found in Reference 10.

While this analysis was based on a dynamic pressure of 100 lb/ft^2 the conservative techniques used in calculating both the stresses and the aerodynamic loads make it possible to safely test up to a dynamic pressure of 200 lb/ft^2.

A. Sting Adapter Components
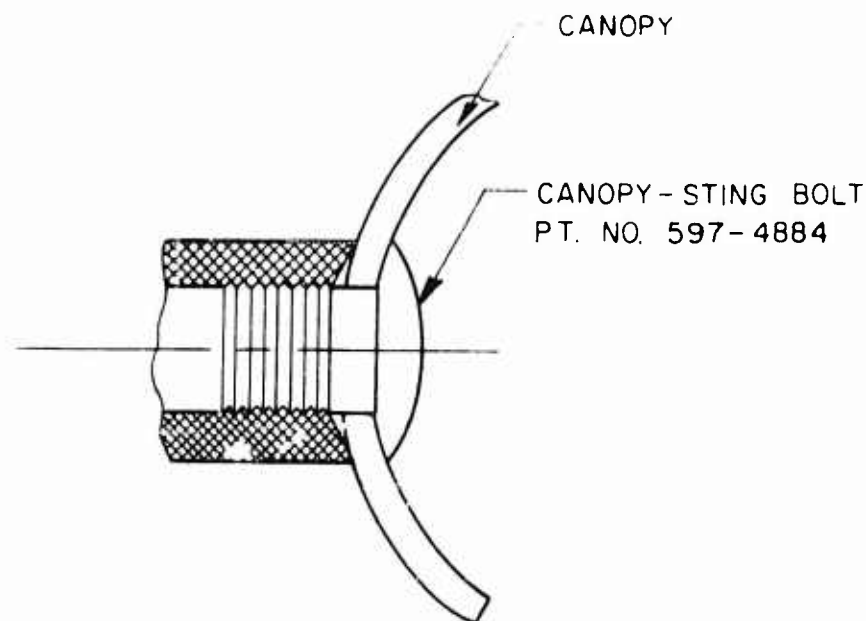
Of the various sting adapter components, the canopy-sting bolt developed the more critical stresses. Below is a free body of this component.
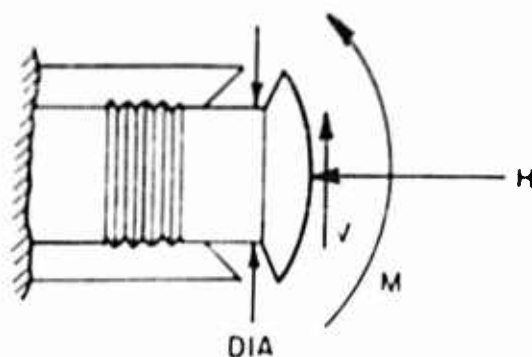
$$M = 218 \text{ in./lb}$$

$$H = 33 \text{ lb}$$

$$V = 22 \text{ lb}$$

$$DIA. = 0.67 \text{ in.}$$

Canopy-Sting Bolt Material - AISI 4130 Steel
Yield Strength - 52000 lb/in^2

The stress developed by the horizontal and vertical forces H and V is not significant and can be ignored. By assuming that the moment M develops pure bending in the bolt, which is not strictly true, but it is conservative to do so; the maximum stress was found from the expression

$$\sigma b = \frac{M}{Z}$$

where

σb = maximum fiber stress

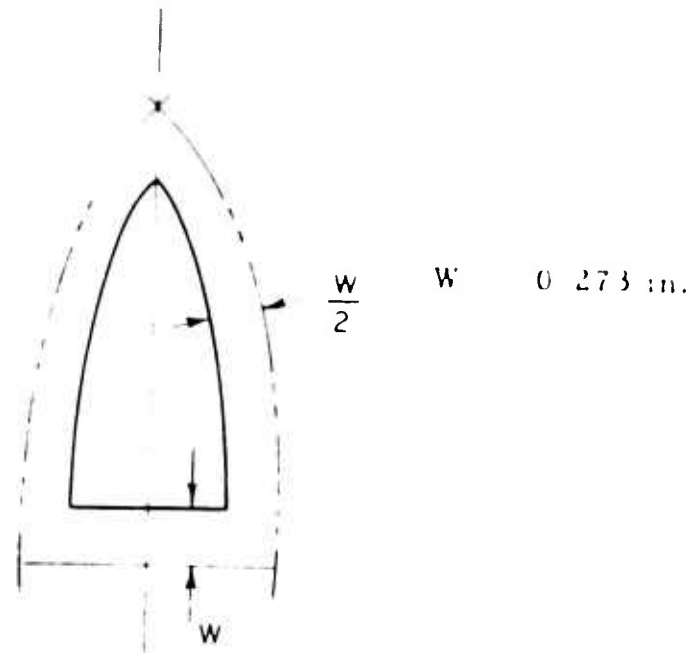M = bending moment

Z = section modulus

Calculations:

$$\sigma b = \frac{218}{0.029} = 7500 \text{ lb/in}^2$$

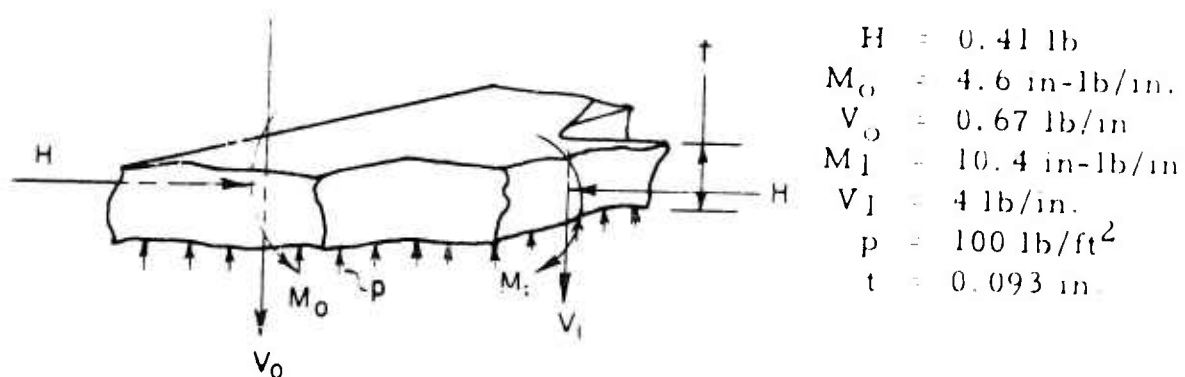$$\text{Safety factor} = \frac{52000}{7500} = 6.9$$

B. Canopy

Of all the canopies considered for testing, the canopy with a gore design as shown below was found to be the most critical.

$$\frac{W}{2} \qquad W \qquad 0.273 \text{ in.}$$

Critical Gore Configuration

This gore is formed from 24 radial ribbons with only one horizontal ribbon located at the mouth or skirt of the canopy.

$$H = 0.41 \text{ lb}$$
$$M_0 = 4.6 \text{ in-lb/in.}$$
$$V_0 = 0.67 \text{ lb/in}$$
$$M_1 = 10.4 \text{ in-lb/in}$$
$$V_1 = 4 \text{ lb/in.}$$
$$p = 100 \text{ lb/ft}^2$$
$$t = 0.093 \text{ in.}$$

Free Body of the Horizontal Ribbon

Canopy Material - 302 Stainless Steel Yield Strength - 80,000 lb/in^2

$$H = 0.41 \text{ lb}$$
$$M_2 = 11 \text{ in/lb}$$
$$V_2 = 4.3 \text{ lb}$$
$$p = 100 \text{ lb/ft}^2$$
$$t = 0.093 \text{ in.}$$
$$R = 4 \text{ in.}$$
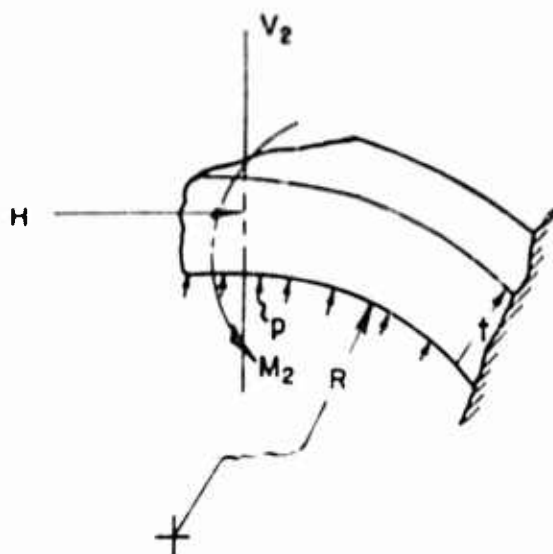
Free Body of the Radial Ribbon

Canopy Material - 302 Stainless Steel Yield Strength - 80,000 lb/in^2

The magnitudes of the moments and forces shown above were obtained from a consideration of the deflection and rotation of the canopy ribbons and the 24 riser lines. To calculate these quantities the horizontal ribbon was treated as a short cylinder and the radial ribbons were considered as thin curved cantilever beams. The 24 riser lines were assumed to be simply supported beams with an edge moment at the canopy end of the lines (see Section C).

1.   Radial Ribbons

The horizontal and vertical forces do not significantly influence the stress in these ribbons and can be ignored. The edge moment M_2 developed a bending stress σb as follows:

$$\sigma b = \frac{M_2}{Z}$$

where

σb = maximum fiber stress
M_2 = edge moment
Z = section modulus

Calculation:

$$\sigma b = \frac{11}{0.0004} = 27,500 \ lb/in^2$$

$$Safety \ Factor = \frac{80000}{27500} = 2.9$$

Ignoring the influence of the riser lines and the horizontal ribbon, the maximum fiber stress in the radials due to the pressure p is given by

$$\sigma = p \frac{R}{t} (1 + \frac{6R}{t})$$

where

σ = maximum normal stress
p = pressure
R = ribbon radius
t = material thickness

Calculation.

$$\sigma = 0.694 \ (\frac{4}{0.094})(1 + \frac{6 (4)}{0.094}) = 7570 \ lb/in^2$$

$$Safety \ Factor = \frac{80000}{7570} = 10.6$$

2. Horizontal Ribbon

Assuming that the horizontal ribbon does not bend or twist, and that each cross section of the ribbon rotates in its own plane about its centroid, the maximum normal stress can be found from the following expression:

$$\sigma = \frac{R}{Z} \left[(V_1 - V_0) \frac{W}{2} + M_1 - M_0 \right] + \frac{R}{Wt} (V_1 + V_0) + p \frac{R}{t}$$

where

σ = maximum normal stress

Z = section modulus

R = ribbon radius

V_1 and V_0 = edge shear/length

M_1 and M_0 = edge moment/length

p = air pressure
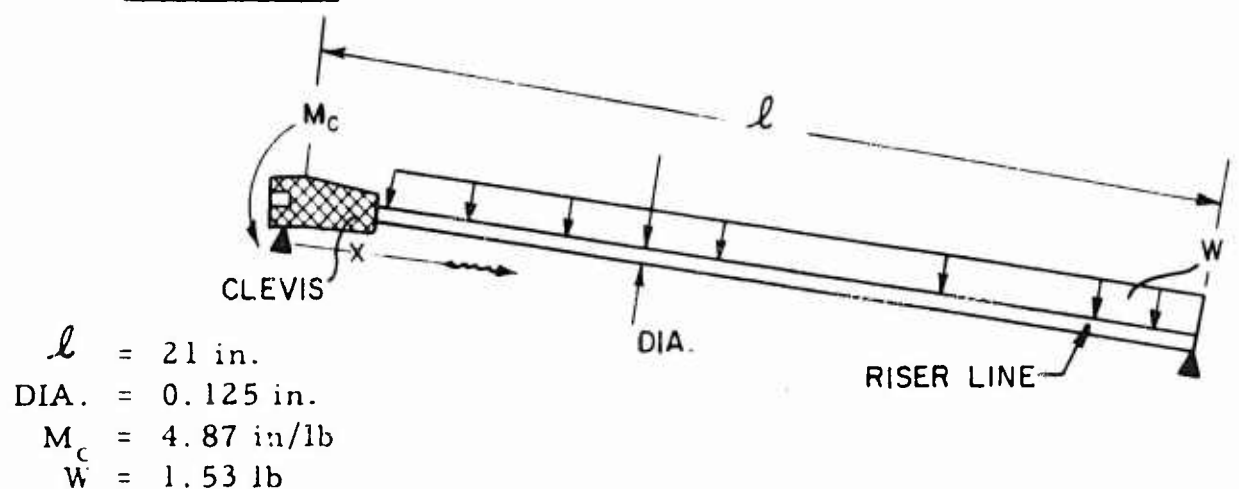
W = ribbon width

t = ribbon thickness

Calculation:

$$\sigma = \frac{4}{0.001164}\left[(4-0.67)\frac{0.273}{2} + 10.4 \qquad 6\right]$$

$$+ \frac{4(4+0.67)}{0.273(0.094)} + \frac{0.694(4)}{0.094}$$

$$\sigma = 22200 \text{ lb/in}^2$$

$$\text{Safety Factor} = \frac{80000}{22200} = 3.6$$

C. Riser Lines

ℓ = 21 in.

DIA. = 0.125 in.

M_c = 4.87 in/lb

W = 1.53 lb

Free Body Diagram of the Riser Lines

Riser Line Material - 440-F Stainless Steel Yield Strength - 100,000 lb/in^2

The total load W was found by assuming that the pressure distribution along the length of the line was uniform. The edge moment M was obtained by using the technique described in Section B. The maximum bending stress at any section can then be found from the following equation:

$$\sigma_b = \frac{1}{Z} \left[\frac{W}{2} \left(X - \frac{X^2}{\ell} \right) - M_c \left(1 - \frac{X}{\ell} \right) \right]$$

where

σ_b = maximum bending stress
Z = section modulus
W = total load
M_c = end moment from the canopy
ℓ = total line length
X = distance to any section

Calculation:

The maximum stress was found at $X = 0.5$

$$\sigma_b = \frac{1}{0.0001918} \left[\frac{1.53}{2} \left(0.5 - \frac{0.25}{21} \right) - 4.87 \left(1 - \frac{0.5}{21} \right) \right]$$

$$\sigma_b = 21600 \; lb/in^2$$

Safety Factor $= \dfrac{100000}{21600} = 4.6$

APPENDIX IV

EXPLANATION FOR REDUCED DRAG AND INFLATION CHARACTERISTICS

Study and analysis of the reduced drag and poor inflation characteristics exhibited in these programs have resulted in the explanatory discussion which is presented in the following pages.

A possible explanation for the occurrence of reduced drag on the parachute in supersonic flow considers that the parachute acts similar to a blunt body with a nose spike mounted ahead of it. The NACA has conducted several programs wherein blunt bodies with attached nose spikes have been tested to investigate means of reducing the drag of supersonic missiles having blunt or rounded noses. Experimental data have been obtained which show that definite decreases in drag result from tests of nose spike-blunt body configurations. Obviously, the flow patterns obtained from such tests were affected by a number of variables such as rod length, cone size, Mach number, and Reynolds number. Other agencies such as the Ballistic Research Laboratories, Aberdeen Proving Ground have conducted similar investigations.

Reference 3 through 6 are reports of some of the tests made by the NACA and Ballistic Research Laboratory. Reference 5, in particular points out the effects which may be achieved by placing a small cone on the end of a rod mounted ahead of the blunt body. Reference 5 explains that the action which takes place when a small cone is mounted symmetrically on a rod ahead of a blunt nose involves the replacement of the strong detached shock wave of the blunt body by a conical shock wave. Figure 16 shows a sketch of typical shock wave patterns for the parachute case as obtained from the Langley test program. This sketch points out the similarity to shock wave patterns of Reference 5 and also illustrates two variations in shock pattern which occurred because of fluctuation and distortion of the shock waves at particular Mach numbers. Shock waves labeled with the number 1 indicate one variation while the other variation is identified by the number 2. The influence of these random variations in shock pattern upon the drag and inflation characteristics is not fully known because drag measurements were not made during the test program at Langley. It is anticipated, however, that the effects are such as to cause further/and varying reductions in the drag and inflation characteristics of the parachutes. The shock pattern designated as number 2 in Figure 16 is assumed for the following explanatory discussion.
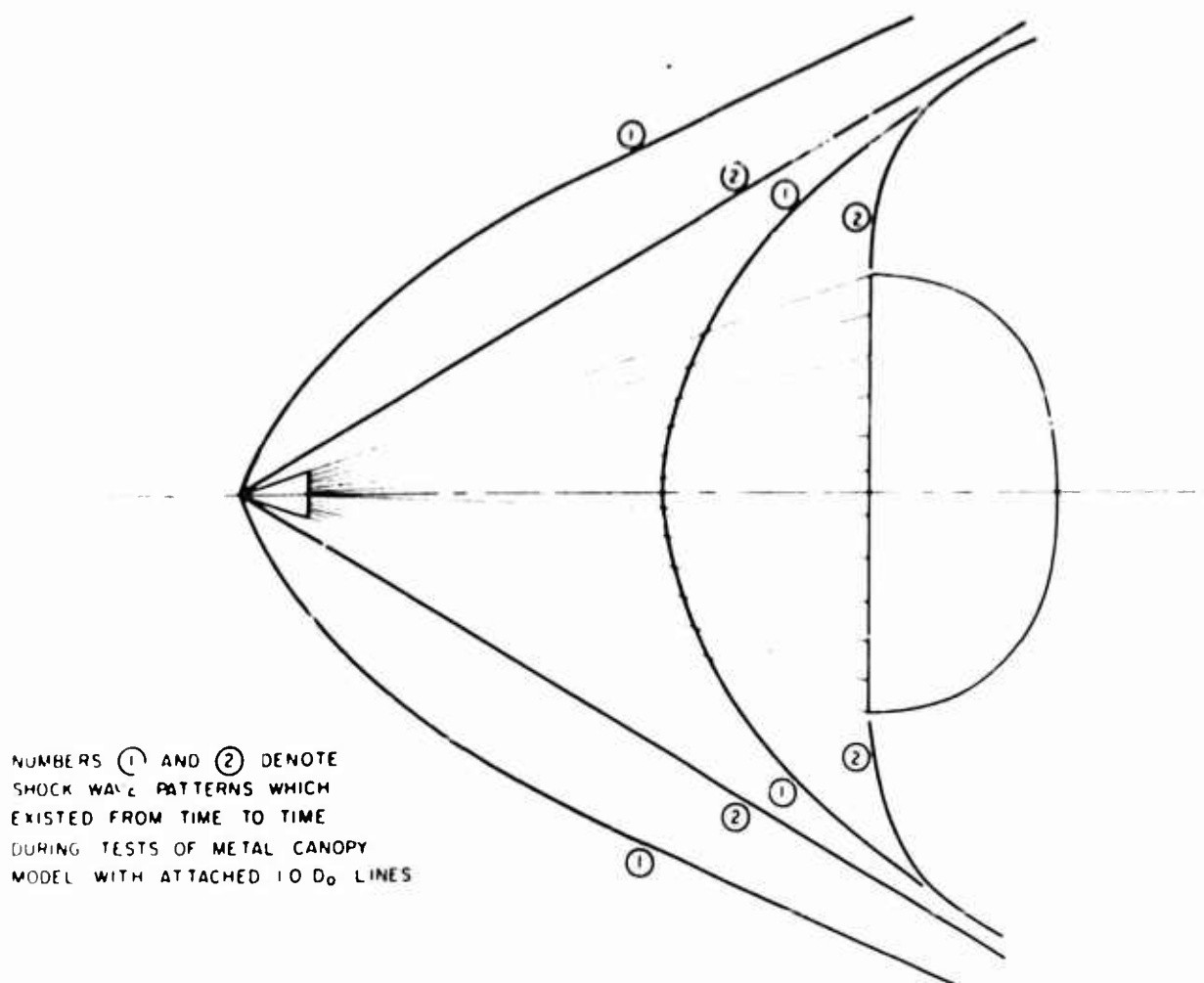
NUMBERS ① AND ② DENOTE
SHOCK WAVE PATTERNS WHICH
EXISTED FROM TIME TO TIME
DURING TESTS OF METAL CANOPY
MODEL WITH ATTACHED 1.0 D_O LINES

Figure 16.   Sketch Showing Two Shock Pattern Variations Occurring at a
Particular Mach Number (Rigid Canopy with 1.0 D_O Lines)

As stated previously, the explanation for the reduced drag experienced
by test parachutes in supersonic flow considers that the parachutes acted
similar to blunt bodies with attached cone-tipped rods. The similarity is
realistic because the metal parachute canopy and attached $1/D_O = 1.0$ steel
rod lines chosen for comparative purposes have a conical nose piece which
holds the lines together at the confluence point. In addition, it can be as-
sumed that comparison of the fabric parachutes tested at Lewis with the
blunt body nose spike configurations of Reference 5 is reasonable since the
suspension lines tend to form a small cone whose apex is identical with the
confluence point. Thus, a flow separation cone is created ahead of the
parachute which by geometry will permit a reasonable comparison with
models of Reference 5.

The Reynolds number of a blunt body with attached cone-tipped rod
(Reference 5) is generally in fair agreement with those of the test para-
chutes. It is reasonable to assume, therefore, that Reynolds number effects

on drag are negligible and that the drag coefficients of Reference 5 are applicable to comparison with the values obtained for the fabric test parachutes.

Before correlation of the drag data of Reference 5 with parachute data could be attempted, it was necessary to establish certain ratios which could provide a means of establishing mutual relationships between the configurations of Reference 5 and the test parachutes. The fineness ratio of the cone or simulated cone in the case of fabric parachutes (lc/dc) and the ratio of the distance between the cone base and body (L/d$_p$) were computed for eight models of Reference 5, five fabric test parachutes and the rigid test canopy with 1.0 D$_o$ lines. These values have been plotted in Figure 18. Sketches of typical configurations which show the pertinent dimensions are also included in this figure.
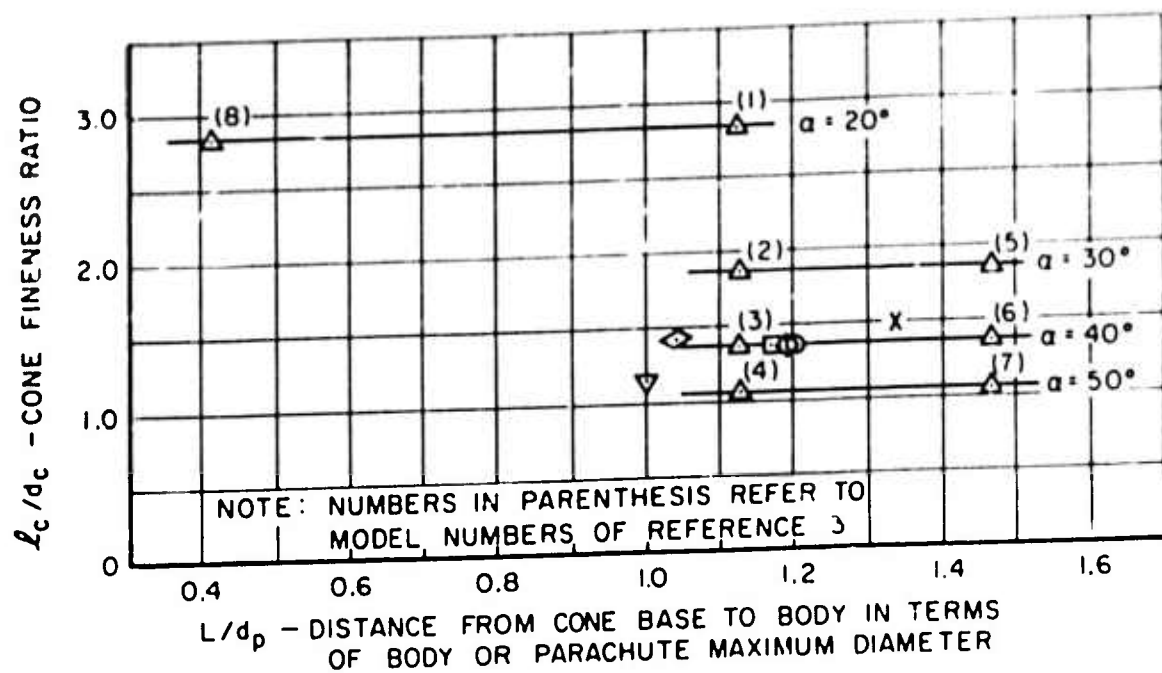
By assuming linear relationships the models of Reference 5 may be represented as shown in Figure 18 by a family of "two point" curves with the cone apex angle as a parameter. It may be seen from Figure 18 that the points plotted for the parachutes are in good agreement with the Reference 5 curves shown. Further examination of Figure 18 indicates that all ribbon test parachutes have points which are in good agreement with the a = 40° curve while the Guide Surface Ribless parachute approaches the 50 degree curve. This corresponds closely with apex angle calculations based on the parachute geometry as represented in Figure 17.

The above and Figure 18 indicate that the comparison of the drag of a ribbon test parachute with that of Model 3 of Reference 5 should be a logical one. Differences in the L/d$_p$ ratios of these parachutes and Model 3 are relatively small. The drag coefficients obtained at a Mach number of 3.5 for four ribbon test parachutes with porosities of 10 to 30 percent varied from 0.20 to 0.34 based on the maximum frontal area of the parachutes. The drag coefficient value of 0.181 given in Reference 5 for Model 3 is in good agreement with the lower end of this range of parachute values but in disagreement with the remainder of the range. It is expected that several factors such as parachute porosity, accuracy of wind tunnel drag data, etc., are largely responsible for the discrepancies between test parachute and
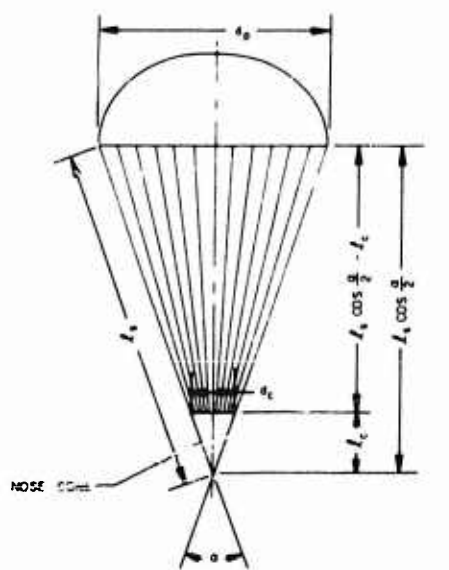
d_p - PROJECTED OR INFLATED PARACHUTE DIAMETER
l_s - SUSPENSION LINE LENGTH
a - APEX ANGLE CREATED BY OUTERMOST LINES
l_c - LENGTH OF NOSE CONE
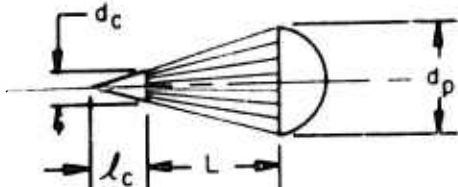d_c - BASE DIAMETER OF NOSE CONE

Figure 17. Parachute Geometry
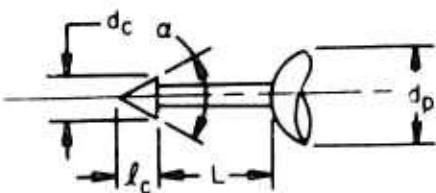
Figure 18. Correlation Ratios for Comparison of Test Parachutes with Cone-Tipped Rod and Blunt Body Configurations of Reference 5

Reference 5 data. The C_D value of 0 181 given for Model 3 was approximately 34 percent of the value obtained for the basic blunt nose of Reference 5. On the basis of the above comparison and depending upon their porosity, the ribbon test parachutes can be assumed to have developed only about 35 to 60 percent of their full drag potential.

APPENDIX V

THEORETICAL METHOD OF DETERMINING CANOPY POROSITY

Theoretical knowledge of the porosity required to achieve flow conditions which yield zero spillover can be obtained by assuming Mach 1.0 flow through the canopy slots. The method and sample calculation which follows illustrates the technique by which the theoretical porosity can be calculated as a function of Mach number. The following sketch may be used to represent the flow conditions.
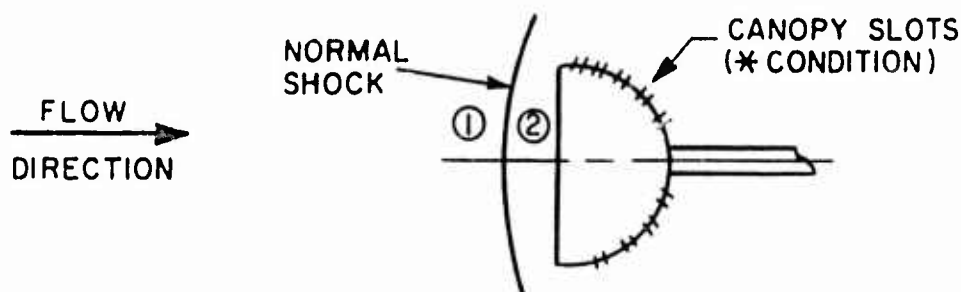
Regions (1) and (2) of the sketch refer to conditions ahead of and behind the normal shock, respectively, while the symbol (*) refers to conditions at the throat or, in this case, at the slots in the canopy. The following symbols are utilized in this calculation:

A = cross-sectional area

V = velocity

ρ = density

T = temperature

M = Mach number

a = speed of sound

λg = geometric porosity

Subscripts 1, 2 or * are used with the above symbols to identify a major symbol with a particular region in the above sketch.

Since the mass flows through the various regions as indicated in the sketch must be the same in steady flow, then

$$\rho_1 A_1 V_1 = \rho_2 A_2 V_2 = \rho_* A_* a_* \tag{1}$$

Since it is desired to determine the slot area (A_*) required to give Mach number 1.0 flow through the slots and since

$$\rho_1 A_1 V_1 = \rho_* A_* a_*$$

then

$$\frac{A_1}{A_*} = \frac{\rho_* a_*}{\rho_1 V_1} \quad \frac{\rho_* a_*}{\rho_1 M_1 a_1} \tag{2}$$

Since $A_* = A_{slots}$ and $A_1 = $ projected or frontal area (A_p) of the inflated parachute, then Equation (2) can be solved for A_* or A_{slots} in terms of A_1 or A_p as follows:

$$A_* = A_{slots} = \frac{A_1 \rho_1 M_1 a_1}{\rho_* a_*} \tag{3}$$

The geometric porosity (λ_g) which is the ratio of slot area (A_{slot}) to the constructed area of the parachute (A_o) can be obtained as follows. Since for ribbon type parachutes,

$$A_1 = A_p \cong \frac{4}{9} A_o$$

then substitution in Equation (3) for A_1 gives

$$A_* = A_{slots} = \frac{4/9\, A_o \rho_1 M_1 a_1}{\rho_* a_*}$$

Rearranging

$$\frac{A_{slots}}{A_o} = \frac{4}{9} \left(\frac{\rho_1}{\rho_*}\right)\left(\frac{a_1}{a_*}\right) M_1 = \lambda_g \tag{4}$$

The solution of Equation (4) for a particular Mach number (M_1) involves the determination of the ratios ρ_1/ρ_* and a_1/a_*. This can be done by utilization of the compressible flow equations and tables of Reference 11. An initial Mach number (M_1) of 3.0 has been considered in the following example. Since the pertinent ratios of Equation (4) cannot be obtained directly from Reference 11, some manipulation is necessary to achieve them. The density ration ρ_1/ρ_* can be obtained from the following expression

$$\frac{\rho_1}{\rho_*} = \frac{\rho_1}{\rho_2} \frac{\rho_2}{\rho_*}$$

The reciprocal of the ρ_1/ρ_2 term can be obtained from Reference 11.

$$\frac{\rho_2}{\rho_1} = 3.857$$

or

$$\frac{\rho_1}{\rho_2} = \frac{1}{3.857} = 0.258$$

The value of ρ_2/ρ_* can be obtained in terms of total density (ρ_+) as follows:

$$\frac{\rho_2}{\rho_*} = \frac{\rho_2/\rho_+}{\rho_*/\rho_+}$$

From Reference 8 then for $M_2 = 0.475$

$$\frac{\rho_2}{\rho_+} = 0.896$$

and similarly for $M_* = a_* = 1.0$

$$\frac{\rho_*}{\rho_+} = 0.634$$

so that

$$\frac{\rho_2}{\rho_*} = \frac{0.896}{0.634} = 1.41$$

therefore

$$\frac{\rho_1}{\rho_*} = \frac{\rho_1}{\rho_2} \frac{\rho_2}{\rho_*} = (0.258)(1.41) = 0.364$$

A value of the a_1/a_* ratio for a Mach number (M_1) of 3.0 can be obtained as follows:

$$\frac{a_*}{a_1} = \frac{a_*}{a_2} \frac{a_2}{a_1} = \sqrt{\frac{T_*}{T_2}} \sqrt{\frac{T_2}{T_1}} = \sqrt{\frac{T_*}{T_1}}$$

The T_*/T_1 term is obtained in terms of T_+ from the expressions

$$\frac{T_+}{T_1} = (1 + \frac{\gamma-1}{2} M_1^2) = \left[1 + (\frac{1.4-1}{2}) \quad (3.0)^2\right] = 2.8$$

$$\frac{T_+}{T_*} = (1 + \frac{\gamma-1}{2} M_*^2) = \left[1 + (\frac{1.4-1}{2}) \quad (1.0)^2\right] = 1.2$$

Therefore

$$\frac{T_*}{T_1} = \frac{T_+/T_1}{T_+/T_*} = \frac{2.8}{1.2} = 2.33$$

and

$$\frac{a_*}{a_1} = \sqrt{\frac{T_*}{T_1}} = \sqrt{2.33} = 1.52$$

The ratio desired is equal to the reciprocal of a_*/a_1 thus

$$\frac{a_1}{a_*} = \frac{1}{1.52} = 0.66$$

Substitution of the pertinent values of ρ_1/ρ_* and a_1/a_* in Equation (4) and solving gives a porosity value for a Mach number of 3.0

$$\lambda_g = \frac{A_{slots}}{A_o} = \frac{4}{9} \left(\frac{\rho_1}{\rho_*}\right)\left(\frac{a_1}{a_*}\right) M_1 = \frac{4}{9}(0.364)(0.66)3.0 = 0.32$$

The above calculation shows that a theoretical porosity of 32 percent is required to achieve zero spillover flow conditions for an initial Mach number of 3.0. Similar calculations for other Mach numbers have given additional porosity values which are represented by the curve shown in Figure 19. Figure 19 shows the variation of calculated geometric porosity with Mach number for a Mach number range of 1.5 to 4.0.
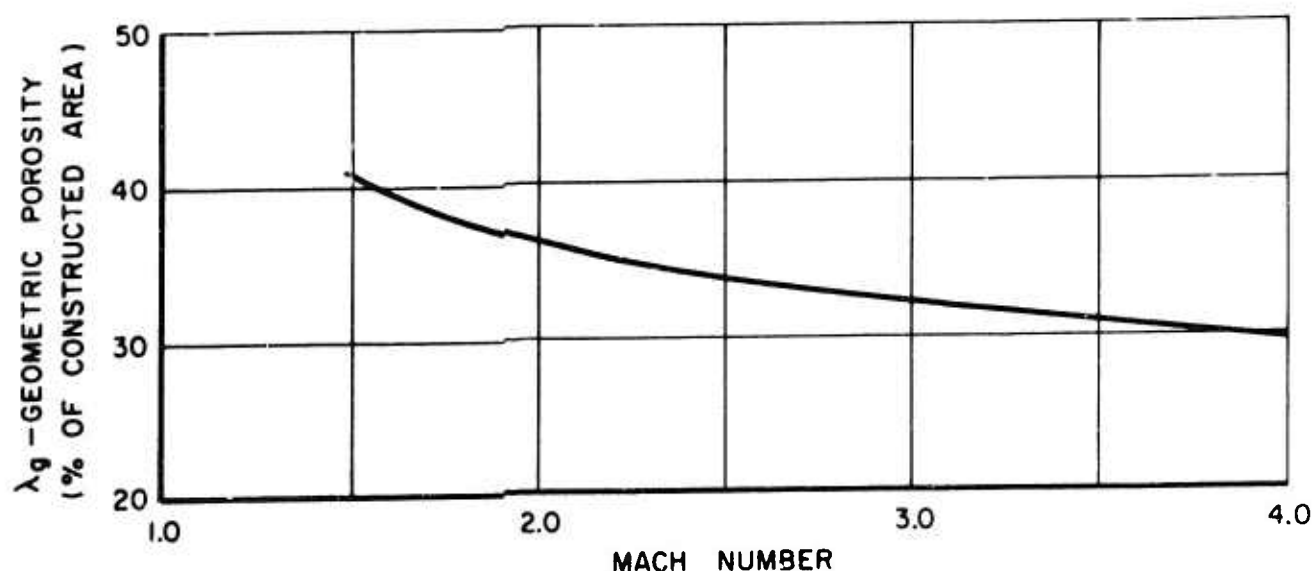

Figure 19. The Parachute Geometric Porosity Required for Zero Spillover as a Function of Mach Number Assuming Mach 1.0 Flow through Canopy Slots